Janne Siren Fjærestad

Hoar frost formation on a salted road surface

Doctoral thesis

Janne Siren Fjærestad

NTNU
Norwegian University of Science and Technology
Thesis for the Degree of
Philosophiae Doctor
Faculty of Engineering
Department of Civil and Environmental
Engineering

NTNU
Norwegian University of
Science and Technology

NTNU
Norwegian University of
Science and Technology

NTNU

Janne Siren Fjærestad

Hoar frost formation on a salted road surface

Thesis for the Degree of Philosophiae Doctor

Trondheim, September 2020

Norwegian University of Science and Technology
Faculty of Engineering
Department of Civil and Environmental Engineering

NTNU
Norwegian University of
Science and Technology

Abstract

Hoar frost formation may lead to slippery driving conditions during late autumn and winter time. Hoar frost formation occurs when humidity in the air deposits directly as ice on the cold road surface. To avoid slippery road during hoar frost situations, anti-icing chemicals are commonly used since they lower the freezing point of water. Unfortunately, the use of chemicals have negative impact on both cars, infrastructure and the environment surrounding the roads. Their usage should therefore be reduces as much as possible, without raising the risk of accidents.

The work of this thesis has been to investigate the process of hoar frost formation on salted road surface. A laboratory setup simulating hoar frost formation has beed developed as a part of this work. It consists of an open loop wind tunnel where warm humid air is forced to flow over a cold stone surface. The setup has shown to be able to simulate hoar frost conditions similar to those reported onsite with sufficient stability on critical parameters, such as temperatures and air humidity.

It is suggested to spilt the process of hoar formation on a salted road surface in two parts, the dilution process and the freezing process. The dilution process occurs from the solution is applied on the road surface until it is diluted to its freezing concentration at the road surface temperature. The time it takes is denoted as the dilution time. The freezing process occurs from the point the freezing concentration is reached until the ice formation results in slippery road conditions. The time it takes is denoted as the freezing time. The time from a chemical is applied on the road surface to the road becomes slippery is denoted the protection time, and it is the sum of the dilution time and the freezing time. Both parts of the process were studied.

The dilution process was studied for solutions of NaCl, $CaCl_2$ and $MgCl_2$. The over all finding was that the presence of anti-icing chemical on the road surface did affect the rate of humidity transport. The presence of anti-icing chemicals did increase the rate up to 30% compared to a surface without chemicals, but the effect diminished during the first two hours as the solution got diluted.

The freezing process was examined for a solution of NaCl. The freezing process was found to start in the top layer of the solution, even though it is colder in the solution/stone interface. This indicates that there is was concentration gradient in the solution due to slower diffusion of water in the salt solution than in the air. A considerable amount of ice could be present on the salted road surface before the ice got strong enough to withstand the simulated mechanical load of traffic. For a film thickness of 0.06 mm of 10% NaCl solution, the critical ice fraction was found to be 0.67. For higher ice fractions the ice was not removed by the pendulum. The critical ice fraction was found to depend on the amount of solution applied, and an ice fraction up to 0.81 was acceptable for an applied film thickness of 0.1 mm.

The increased mass flux due to the presence of chemicals contributes to a reduction in the

protection time. Opposite, the critical ice fraction contributes to an extension in the protection time. Calculations have shown that by including the freezing period, the total protection time is more than 3 times longer than estimated when assuming that the protection time ends when the freezing concentration is reached. When including the increased mass flux in the dilution period, the total protection time is reduced by only 5-7% of the protection time calculated without the increased mass flux.

Preface

This thesis is submitted to the Norwegian University of Science and Technology (NTNU) for partial fulfillment of the requirement for the degree of philosophiae doctor (PhD).

This doctoral work har been performed at the Department of Civil and Transport Engineering, NTNU, Trondheim, with Professor Alex Klein-Paste as the main supervisor and PhD Johan Wåhlin as co-supervisor.

This PhD project was funded by the Norwegian Public Roads Administration (NPRA) and was initiated as a part of the E39 coastal highway route along the west coast of Norway.

Acknowledgment

First of all I would like to thank my two supervisors Alex Klein-Paste and Johan Wåhlin for sharing of their great knowledge and letting me in to the field of winter maintenance. Thanks for all the support and guidance in all phases of the work. This work would not have been possible without you.

I would also like to thank Bent Lervik, Per Asbjørn Østensen, Frank Stæhli and Tage Wessum for providing necessary parts of my lab equipment whenever needed. Special thanks to my friends and colleagues at the VTG lunch room. You have all made my time at NTNU enjoyable.

Last but not least; thanks to my friends and family for the support during this period. Thanks to my three lovely kids, Vegard, Eline and Sigrid, for always giving me reasons to smile, and finally, a special thank to Håkon for all your love, support and patience.

Trondheim, March 31, 2020

Janne Siren Fjærestad

Contents

Contents

Chapter 1

Introduction

1.1 Background

During winter time, roads and bridge decks can become slippery due to hoar frost on the road surface and create dangerous conditions for motorists (Norrman et al., 2000). In Sweden in the winters of 2004-2005 and 2005-2006, 18.1% and 14.5% of accidents respectively, occurred during hoar frost formation (Andersson and Chapman, 2011). Hoar frost growth occurs when water vapor in the air goes directly from gaseous state to solid state on a cold surface. For a surface without any anti-icing chemicals this can occur when the surface has a temperature below both the dew point temperature and the freezing temperature of water.

Two typical situations where hoar frost formation occurs are 1) when warm, humid air flows over a cold road surface and 2) when the road surface is cooled further down by large outgoing long wave radiation during clear sky conditions. The former phenomenon is the most frequent cause of hoar frost in Northern Sweden, while in Southern Sweden the second phenomenon is the most frequent cause (Ou et al., 2019). Bridges cool more rapidly than adjacent roads (Knollhoff et al., 1998), and they are therefore more vulnerable to hoar frost formation. The Norwegian Public Roads Administration (NPRA) is planning for an upgrade of the E39 highway route at the westcoast of Norway. This includes replacing ferries by bridges for several fjord crossings along this route. Knowledge about how to avoid slippery roads due to hoar frost formation on bridges is therefore valuable for the E39 project.

Different actions can be made to reduce the risk of fatalities due to hoar frost formation. This includes the application of anti-icing chemicals, heating of the bridge deck, sensing and warning for hoar frost conditions and the use of high friction overlays on the top surface of the bridge deck. The three former actions all require good knowledge about both present and expected future surface conditions in order to be used in an efficient and safe way. Several socalled road weather models that predict the surface temperature and the surface state (e.g. dry, wet, snowy, icy) on both roads and bridge decks already exist (e.g. Sass (1992); Crevier and Delage

(2001); Knollhoff et al. (2003); Greenfield and Takle (2006)). In addition the models by Denby et al. (2013) and Fujimoto et al. (2014) also includes the presence of chemicals on the road surface. However, little is known about how the presence of anti-icing chemicals affect the process of hoar frost formation and when the deposited hoar frost actually leads to slippery conditions.

Anti-icing chemicals is the main method to prevent hoar frost formation. Unfortunately, chemicals have a negative impact on the environment (Ramakrishna and Viraraghavan, 2005; Fay and Shi, 2012) and can cause corrosion of vehicles, equipment and infrastructure, such as bridges (Shi et al., 2014; Li et al., 2013; Xu and Shi, 2018). To reduce these negative effects and enhance the infrastructure lifetime, chemicals should be used only when needed and in the right amounts. This requires knowledge about how chemicals influence the process of hoar frost formation, and how long they prevent the road from becoming slippery during a hoar frost situation.

1.2   Research objectives

Anti-icing chemicals are used to avoid hoar frost formation on roads and bridge decks during late autumn and winter time. The chemicals lower the freezing temperature of water, and are used to keep humidity transported to the road in a liquid state. The presence of anti-icing chemicals also changes the water vapor pressure at the surface, which may impact on the humidity transport between the air and the road surface (Denby et al., 2013). If humidity is transported to the road, it will reduce the concentration of the applied chemical and the freezing temperature will increase. If freezing occurs, the road might get slippery. However, little is known about how the process of hoar frost formation progresses on a salted road surface.

The objective of this thesis has been to deeper understand this process of hoar frost formation on a salted road and to gain knowledge necessary to predict if the salted road surface will get slippery during a hoar frost event. This included the following sub-objectives:

- Establish a laboratory setup for simulating hoar frost formation on a road surface.

- Examine how typical anti-icing chemicals affect the humidity transport between the air and the road surface.

- Examine how the hoar frost formation process progresses on a salted road surface.

- Determine if and when hoar frost makes a salted road slippery.

1.3   Approach

This thesis is mainly based on experimental work. An experimental setup was designed, built and tested in order to simulate hoar frost formation in the cold walk-in laboratory at the Winter Maintenance Centre at NTNU. This work resulted in Paper I. The process of hoar frost formation on a salted road surface were examined in two studies performed using the setup. Paper II focuses on how the presence of NaCl, CaCl$_2$ and MgCl$_2$ influences the humidity transport between the air and the road surface during conditions for hoar frost formation. Paper III focuses on how freezing occurs on a salted road surface during conditions for hoar frost formation. In addition, some theoretical work has been done in order to study how existing thermodynamic theory combined with an activity model for aqueous solutions can be used to determine the direction of the humidity transport between the surface and the air for a salted road surface. This work is included as a part of Paper IV.

1.4   Thesis structure

This thesis consists of 6 chapters. In addition, the four papers are included in the Appendix. Chapter 1 provides the introduction to the problem, including research objectives, approach and an overview of the papers published. Chapter 2 gives an introduction to the process of hoar frost formation and the most important winter maintenance strategies during hoar frost situations. The research methods used are described in Chapter 3. This includes the process of developing the laboratory setup, the method to test the mechanical strength of the ice and the theoretical work to related to the direction of the humidity transport. Detailed information about how the different hoar frost tests were performed can be found in the respective papers. Chapter 4 presents the main results from the work, separated into the four different papers. In Chapter 5 the results are discussed. The discussion is separated in three parts: 1) the performance of the laboratory setup, 2) the total hoar frost formation process and 3) how the findings from this thesis contributes to knowledge needed to chose what type and amount of chemical to be used prior a hoar frost event. Finally, in Chapter 6, the main conclusion of the thesis is presented together with suggestions for future work.

1.5   Papers

The papers that have contributed to the results of this thesis are briefly described in this section.

Paper I

Experimental setup simulating hoar frost formation on roadways

Fjærestad, J. S., Wåhlin, J. and Klein-Paste, A. (2020). Journal of Cold Regions Engineering.
https://doi.org/10.1061/(ASCE)CR.1943-5495.0000207

This paper describes the design and performance of a setup to simulate hoar frost formation on roadways. The setup was able to produce conditions similar to those of hoar frost formation on a roadway with good stability. The hoar frost growth rates were found to be within the range of field measurements earlier published.

My contribution to this work was to lead the development process, perform all experimental work, data analysis and writing the paper. Johan Wåhlin contibuted with ideas during the concept work, practical help and advices during testing and scientific discussions during the data analysis and writing phases. Alex Klein-Paste contributed to the research idea and the concept behind the setup. He also contributed with scientific discussions and advises during both the data analysis and writing phase.

Paper II

The effect of anti-icing chemicals during hoar frost situations

Fjærestad, J. S., Wåhlin, J. and Klein-Paste, A. (under review). Journal of Cold Regions Engineering

This paper examines how three commonly used anti-icing agents affect the humidity transport between the air and the road surface during conditions for hoar frost formation. The chemicals were seen to increase the mass flux towards the road surface up to 30% in the start of the dilution process. The effect quickly diminished and after only 60 minutes it returned to a similar rate as without any chemical present.

My contribution to the work was to perform all tests, performing data analysis and writing the paper. Johan Wåhlin contributed with advices during the data analysis and scientific discussions. Alex Klein-Paste contributed with the idea of this study and scientific discussions during the writing phase.

Paper III

Chemical Frost Protection of Road Surfaces: A Laboratory Investigation

Fjærestad, J. S., Klein-Paste, A. and Wåhlin, J. (2020). Transportation Research Record: Journal of the Transportation Research Board.
https://doi.org/10.1177/0361198119900122

This paper examines how freezing occurs on a salted road surface during conditions for hoar frost formation. It is shown that a salt solution diluted by humidity transport from the air starts to freeze from the top despite that the heat is extracted from the bottom. The mechanical strength of the resulting hoar frost is tested, and it is found that a certain amount of ice can be allowed without resulting in slippery driving conditions.

My contribution to the work was to conduct the experiment, performing data analysis and writing the paper. Alex Klein-Paste contributed with the idea of this study, practical advises when testing the mechanical strength of the ice and scientific discussions during the writing phase. Johan Wåhlin contributed with practical help during the experimental work and scientific discussions during the writing phase.

Paper IV
Thermodynamics of deicing chemicals

Wåhlin, J., Fjærestad, J. S., Thomsen, K. and Klein-Paste, A. (2017). TRB 96th Annual Meeting Compendium of Papers.

This paper describes how existing thermodynamic theory combined with an activity model for aqueous solutions can be used to calculate properties relevant for winter maintenance. Three common chloride salts, NaCl, $MgCl_2$ and $CaCl_2$ were studied, and the extended UNIQUAC model was used to acquire the water activity for solutions of the three salts and mixes thereof. With the activity we could find the most stable state (solid, liquid as solution or vapor) of water at different temperatures. Two examples of applications for winter maintenance are presented, one predicting whether humidity will condensate on or evaporate from the road surface after applying anti-chemicals and the other calculating the ice melting capacity and freezing point of the salt solutions.

My contribution to the work was the calculations related to and writing of the "Solution-Air Interaction" section. Johan Wåhlin contributed with the idea of this paper, the major part of both theoretical considerations, calculations and writing. Kaj Thomsen contributed with access to the UNIQUAC model and description of the model. Alex Klein-Paste contributed to reviewing and commenting the manuscript.

Chapter 2

Hoar frost formation

This chapter provides an introduction to the process of hoar frost formation, together with the most important winter maintenance strategies to avoid fatal accidents due to hoar frost formation.

2.1 Hoar frost formation

Hoar frost occurs when water molecules goes directly from a gaseous state in the air to a solid state on a cold surface. This can occur when the surface temperature is lower than both the dew point and the temperature at which water freezes. The mechanism behind this mass transport is the difference in the energy state for water molecules in the air and at the frost surface. Water molecules will prefer the state with the lowest energy. The rate of the resulting hoar frost growth can be described using different driving potentials, for example partial vapor pressure, molar density, and mass density (Webb, 1990). In this work the partial water vapor is used as driving potential, according to the models by Knollhoff et al. (2003) and Denby et al. (2013). The rate of the resulting frost growth can then be described as:

$$\dot{m} = K_p(p_{v,a} - p_{v,fs}) \tag{2.1}$$

where K_p is the mass transfer coefficient, $p_{v,a}$ is the water vapor pressure in the air and $p_{v,fs}$ is the water vapor pressure at the frost surface.

A commonly used assumption in frost formation models is that the air is saturated at the frost surface (Kandula, 2011). It has been found that this assumption leads to an over prediction of the frost growth rate (Na and Webb, 2004), as a certain degree of supersaturation is needed for hoar frost to form. The required degree of supersaturation depends on the surface energy and hence the contact angle, due to lack of this information the assumption used by other hoar frost formation models is kept in this work. The water vapor pressure at the frost surface, $p_{v,fs}$, is

therefore given as the saturation vapor pressure for the surface temperature, T_s. The saturated
vapor pressure over ice is plotted in Figure 2.1. It is seen that the saturation pressure decreases
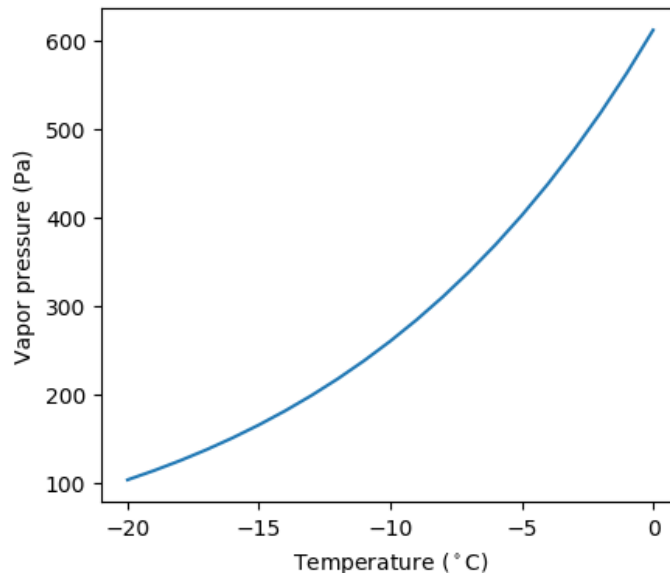for decreasing temperatures.

Figure 2.1: Saturated vapor pressure over ice. Values are calculated according to Murphy and
Koop (2005).

From Eq. (2.1) it is seen that the rate of the frost growth will be increased by lowering the road
surface temperature. This explains why the larger cooling rates for bridges (Knollhoff et al., 1998)
makes them more vulnerable for hoar frost formation than adjacent roads, possibly resulting in
hoar frost on the bridge while the adjacent road remains clear. Such sudden changes in the
driving conditions has lead to fatal accidents (SHT, 2010).

As already mentioned, hoar frost formation may occur under different weather phenom-
ena. Hoar frost formation during clear sky conditions have been simulated with a cold ceiling
to achieve the needed long wave radiation loss from the surface as described by Stanton et al.
(2012). Cheng (2003), Hermes et al. (2009) and Kandula (2012) have all simulated hoar frost for-
mation with warm humid air flowing over a cold surface. Common for these experiments is that
they produce hoar frost at much higher rates than realistic for road situations. The air tempera-
tures were typically between 15 to 25 °C, and the frost surface temperatures were between −5 to
−20 °C.

2.2 Winter maintenance strategies

Different winter maintenance strategies are used to avoid accidents due to slippery driving conditions during hoar frost situations. The different strategies are described later in this section. In order to ensure safe and efficient use, several of them requires good knowledge about both present and future expected road surface conditions. To cover this need, numerous models have been developed to predict both the road surface temperature and the surface state (i.e. dry, wet, snowy, icy) e.g. (Sass, 1992; Crevier and Delage, 2001; Knollhoff et al., 2003; Greenfield and Takle, 2006; Denby et al., 2013; Fujimoto et al., 2014) based on data from road weather information systems (RWIS) and road weather forecasts.

Anti-icing chemicals

Applying salt or other chemicals is common to minimize the risk of slippery roads during wintertime. Typical salts and chemicals used are Sodium Chloride (NaCl), Magnesium Chloride (MgCl$_2$), Calcium Chloride (CaCl$_2$), Magnesium Acetate (CMA) and Potassium formate (KCOOH). The use of chemicals in winter maintenance has mainly been explained by their freezing point depression. The freezing point of water is lowered when foreign molecules or ions are dissolved (Atkins and Paula, 2006). This allows water to be present in a liquid state, also for temperatures below 0°C.

Prior and during hoar frost situations chemicals are used to prevent slippery driving conditions. Such proactive application is referred to as anti-icing (Minsk, 1998). The preferable method for this is by using liquid solutions, since it allows the salt to be applied uniformly over the pavement at relatively fast spreading speeds. Solutions can also be applied on a dry surface without being removed by blow-off (Ketcham et al., 1996).

The timing of an anti-icing application is important. If application is performed too early, salt will be removed by traffic before the hoar frost situation occurs. If application is performed too late, the road may become slippery. Since the road network is divided into routes (ranging from 20 to 60 km) that are served by a single maintenance truck, a future hoar frost situation has to be predicted early enough to allow the truck to cover the entire route before the road gets slippery. In additions, the applied chemical has to be able to keep the road free of ice until the maintenance truck is able to pass a second time. It should be mentioned that for specific critical parts of the road network, such as bridges, Fixed Automated Spray Technology (FAST) systems can be used to keep the road clear of hoar frost, snow and ice. Such systems automatically applies anti-icing chemicals on the road surface, and consists of tanks, pumps, filters and nozzles (Friar and Decker, 1999). The systems can be activated using analysis of real-time data describing the weather and road surface conditions at the site (Hanson et al., 2013). However, most bridges do not have such systems and rely on "traditional" chemical application using

maintenance trucks.

Model prediction of road surface conditions is challenging, as the road surface conditions will strongly depend on the presence of anti-icing chemicals. In addition, the chemicals also influence on the water vapor pressure at the surface, which my impact on the humidity transport between the air and the road surface (Denby et al., 2013). The models by Denby et al. (2013) and Fujimoto et al. (2014) include the impact of NaCl on the water vapor pressure at the surface, to improve the modeled humidity transport. Denby et al. (2013) did find a positive effect on the prediction of road moisture conditions when including the salt impacts. However, these models are complex and include several effects such as e.g. traffic, precipitation, and salt loss mechanisms. Examining the hoar frost process itself and how different chemicals affect it, is not a part of these studies. To the best of my knowledge, little is actually known about how the specific process of hoar frost formation occurs on a salted road surface. Examining this process in a laboratory will therefore be valuable in order to determine what amounts and types of chemicals should be used during hoar frost situation.

Thermal methods

Thermal methods can also be used for specific spots, like bridges, to keep the road surface temperature above $0\,°C$ (Minsk, 1998). Thermal methods include both hydronic and electrical systems. Hydronic systems is built of a pipe network embedded in the pavement and thermal energy is added to the road surface by the circulation of a warm fluid (Johnsson, 2017). Different electrical systems exists, i.e. electrical conductive concrete, electrical resistive heating and infrared heating (Zhang et al., 2009). The energy demand for thermal heating is considerable. To reduce both the environmental impact and the operational costs the use should therefore be optimized. Optimized use can be related to what road surface temperature is needed. By keeping the temperature above $0\,°C$ neither snow, ice or hoar frost will stay on the road. However, in order to avoid hoar frost on a dry road, keeping the road surface temperature above the dew point temperature could be sufficient. Another way of reducing the environmental consequences for thermal systems is to use renewable energy sources. Examples of this includes solar or wind powered electricity (Zhang et al., 2009) and seasonal storage of solar collected thermal energy (Johnsson, 2017).

Friction overlay

Another method to provide safer driving conditions on bridges is placing high friction overlays (HFO) on the bridge decks. A high friction overlay is a thin overlay that consists of fine aggregates embedded into an epoxy or asphalt bonding matrix (Dave et al., 2017). The usage of these overlays has two purposes; to prevent infiltration of water and aggressive chemicals into the bridge

decks and supporting structure, and to increase the skid resistance. Two examples of epoxy based overlays are the SafeLane^{TM} System (Cargill, Incorporated) and the POLY-CARB FLEXO-GRID System (POLY-CARB). Both systems promise to protect the underlying construction and to provide a skid-resistant surface. In addition, the SafeLane^{TM} system provides greater residual effects for the anti-icing product by storing the anti-icing and deicing chemicals in the surface and then releases them when needed.

Evans (2010) has evaluated the of SafeLane^{TM} for crash reduction on bridge decks. He concludes that reduced accident rates are found and attributes this directly to improved traction and indirectly to the retention of chemicals. Dave et al. (2017) have studied the performance of different High Friction Bridge Deck Overlays on bridge decks in Minnesota. They concluded that HFO systems do provide an increase in surface friction. However, due to the lack of relation between the skid number (a measure of friction) and crash rates, they question whether the skid number may be a reliable indicator of crash-rate reduction. They were not able prove with their data that the reducing trend in numbers of crashes were related to the installation of HFO systems.

Monitoring of surface conditions and warning

Another way of reducing the risk of fatalities due to hoar frost formation is to use a warning system. Such systems typically consists of sensors that can detect when there is a high risk of slippery conditions together with dynamic signs that provide motorists real-time warning about slippery road conditions (Veneziano et al., 2014). The underlying principle is that such systems are supposed to alert drivers to observe road conditions more carefully, to provide information about dangerous conditions that are not easily detectable, and to motivate drivers to obey posted speed limits (Rämä and Luoma, 1997). It has been reported that the vehicle speeds are lower when the warning sign is on (Veneziano et al., 2014), and the same effect was found when warning signs were combined by dynamic signs with variable speed limits (Rämä, 1999). Optimized used of such systems also requires good knowledge about when the road surface actually is slippery.

Chapter 3

Research methods

This thesis is primarily based on experimental work. This chapter describes the process of developing a suitable experimental setup to study hoar frost formation on a road surface. The detailed specifications and usage of the setup is described in Paper I, II and III, and is therefore not presented here. In Paper III, a method to determine at whether or not the road is likely to be slippery, for a given hoar frost formation was used. This method, and its adaptations from from earlier studies is described. Finally, the theoretical work with combining thermodynamical theory with an activity model for aqueous solutions from Paper IV is described.

3.1   Hoar frost formation

In order to study the process of hoar frost formation on a salted road surface, it is valuable to be able to simulate the process in a laboratory. Laboratory experiments allow to control important parameters, such as air temperature, surface temperature and relative humidity in the air.

A concept based on an open loop wind tunnel was chosen as it provides good control of the wind speed. The wind tunnel was made by polycarbonate in order to allow visual inspections of the process during the tests. This excluded the possibility to simulate hoar frost formation due to large outgoing long wave radiation. Cooling from the ceiling above would also cool the roof and the walls of the wind tunnel, resulting in har frost formation inside the wind tunnel. The concept of letting warm humid air flow over a surface cooled from below was therefore chosen. Humidity was added to the air by forcing the air over a bath of warm water, and the surface of hoar frost formation was cooled by Peltier elements. A sketch of the setup can be seen in Figure 3.1. The build-up of hoar frost took place on an 80 mm x 80 mm stone with a height of 9 mm. Typical asphalt concrete consists of 95% stone and 5% mastic, which is bitumen and filler. Therefore, it was decided to use a stone in order to achieve an even heat transfer through the test sample and to avoid potential artifacts due to the presence of mastic.

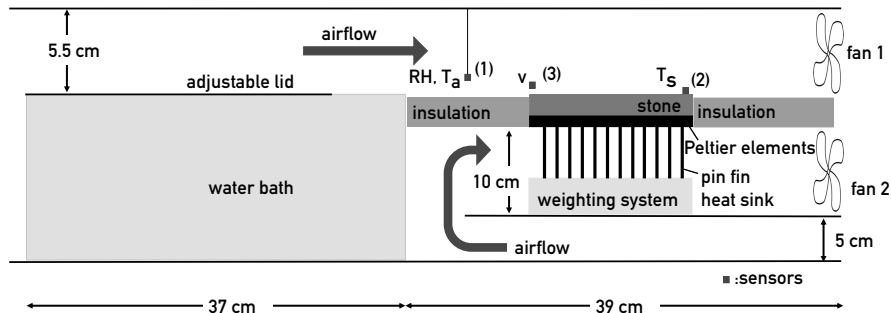During the design of the setup we aimed to perform continuous weight measurements of the

Figure 3.1: Sketch of experimental setup showing how humid air flows over the cold stone surface resulting in hoar frost formation. Sensor 1 measures RH and T_a and is located 9 cm in front of the stone at a height of 2.5 cm above the stone surface. Sensor 2 measures T_s and is located at the corner of the stone. Sensor 3 measures wind speed and is located in front of the stone at a height of 1.5 cm.

added humidity during the tests. This feature would allow to study how the rate of the humidity transport was changing, both during the dilution process and the freezing process, without disturbing the air flow by opening the wind tunnel. As seen in Figure 3.1, both the stone itself and the cooling system, consisting of Peltier elements and a cooling rib, had to be placed on the weighting system. The total weight of this was ~700 g. The addition of water to the stone surface is a rather slow process, and the expected total mass of added water was 2-3 g over a time period of around 10 hours. To measure such small changes to a large mass turned out to be very challenging. A first attempt to solve this, was by using two load cells. The cooling system and the stone was mounted on one load cell, and a weight of same mass was mounted on the other load cell. Both load cells were placed inside the cooling loop of the setup, securing equal wind, temperature and humidity conditions. The idea was to be able to compensate for both creep in the load cell material and drift related to humidity and temperature variations. Unfortunately, this did not work out, and different behavior when exposing both load cells to static loads during tests was observed.

The next attempt was to use a regular electronic scale. This was also placed inside the cooling loop, and therefore exposed to challenging wind conditions. This setup showed promising results when exposed to static load over time and it was used during the hoar frost test presented in Paper I. For all tests in this experiment the stone was weighted manually on another electronic scale before and after hoar frost formation. This revealed unsystematic deviation between the two methods. The deviation did not correlate with the temperature or the duration of the tests. We suspect that the scale has unknown drift-compensating algorithms that made the scale unable to accurately record a slowly increasing mass, without the possibility to "zero" the

scale. The experiment examining the dilution process (Paper II) was therefore done by manually removing the stone from the wind tunnel every 10th minute, in order to examine how different anti-icing chemicals affect the rate of the humidity transport from the air to the road surface.

3.2   Mechanical strength of hoar frost

In order to determine the protection time of an anti-icing action, it is necessary to know when the road gets slippery. For the system of an anti-icing chemical and water, ice and solution can coexist for temperatures above the eutectic temperature and concentrations below the liquidus line. The ice fraction describes the amount of ice present in the system, i.e. the mass of ice divided by the total mass of ice and solution. The ice fraction can be found from the phase diagram of NaCl using the lever rule:

$$F_{ice}(T) = 1 - \frac{c}{c_f(T)} \tag{3.1}$$

where c is the calculated concentration of the solute on the stone surface, i.e. the mass of added chemical divided by the total mass of chemical and water. $c_f(T)$ is the freezing concentration at the surface temperature. Hence $F_{ice} = 0$ means that everything is liquid and $F_{ice} = 1$ means that everything is frozen.

For wet pavement anti-icing it has been reported that a much lower salt concentration than found from the freezing curve is enough to keep the friction at acceptable levels (Haavasoja et al., 2012; Klein-Paste and Wåhlin, 2013). This means that a certain amount of ice ($F_{ice} > 0$) can be allowed on the road surface when anti-icing chemicals are present, without resulting in slippery driving conditions. The explanation for this is that the anti-icing chemicals reduce the mechanical strength of the ice forming, and the ice is therefore destroyed by traffic. Similar to Klein-Paste and Wåhlin (2013) a British Pendulum Tester (Giles et al., 1964) has been used in this work to simulate the mechanical load of traffic. Tests were performed on samples with different ice fractions in order to find the critical limit. Each test sample was exposed to five pendulum passes before they were visually inspected in order to determine the amount of hoar frost removed by the pendulum. The width of a standard rubber block was reduced to 40 mm to ensure the block did not touch the silicon rim and the temperature sensor. Due to the air temperature of 2 °C, the pendulum tests was performed in a neighboring cold room. Here the air temperature was −5 °C, which is close to the stone surface temperature.

3.3   Thermodynamics of anti-icing chemicals

The purpose by using chemicals in winter maintenance is to change or control the properties of any water present on the road surface. Chemicals are added for example to melt ice or to keep water present on the road in a liquid state. The preferred state for the water in a given solution (i.e. solid, liquid, vapor) can be determined by looking at the chemical potential of water. Water will always prefer the state with the lowest chemical potential. The value of the chemical potential always refers to a specific substance. For a given substance, it also depends on temperature, pressure, the concentration and the kind of solvent, and the phase (Job and Herrmann, 2006). The chemical potential of water in a solution, μ_w^{sol}, can be expressed as:

$$\mu_w^{sol} = \mu_w^{water} + RT \ln a_w^{sol} \tag{3.2}$$

where water is used as reference state, and μ_w^{water} is the chemical potential of water as pure water. T is temperature and R is the gas constant. a_w^{sol} is the activity of water in the solution. The water activity in the solution is given as the ratio between the water vapor pressure of the solution and water vapor pressure of pure water under the same conditions (Koop et al., 2000):

$$a_w^{sol} = \frac{p^{sol}}{p^{water}} \tag{3.3}$$

The water activity is often described as the amount of free water, not bond to dissolved chemicals. The water activity ranges from 0 for no free water to 1 for pure water. In this thesis, the Extended UNIQUAC model (Thomsen, 2005) has been used to acquire water activity data for solutions of NaCl, $CaCl_2$ and $MgCl_2$. The model is valid from the freezing points of the solutions to 110°C.

Similarly to Eq.(3.2) the chemical potential of water as vapor, μ_w^{vap}, and as ice, μ_w^{ice}, can be expressed as:

$$\mu_w^{vap} = \mu_w^{water} + RT \ln a_w^{vap} \tag{3.4}$$

$$\mu_w^{ice} = \mu_w^{water} + RT \ln a_w^{ice} \tag{3.5}$$

At a certain temperature it is seen from Eqs.(3.2)-(3.5), that the only difference is the water activity of the respective state. It is seen that the chemical potential is lower the lower the water activity is. Based on this it is possible to determine if water will condense to the solution or if it will evaporate to the air by comparing the water activity of the solution with the water activity of vapor. According to Eq.(3.3) the activity of water vapor in the air is equal to the definition of relative humidity of the air. RH $> a_w^{sol}$ therefore means that water will be transported from the air to the solution. In the same way, it is possible to predict if the water in a solution will freeze or

stay liquid, by comparing the water activity for ice with the water activity for the specific solution at the given temperature.

In paper IV, this methodology was used to determine under which conditions water will condensate to different anti-icing chemicals, and vice versa, what conditions is needed to dry up the road.

Chapter 4

Results

This chapter presents the main results of the thesis. The results are divided into the four different papers.

4.1 Simulating hoar frost formation - Paper I

In total 15 frost growth tests were performed. Ten were performed with an air temperature of $2\,°C$, and five with an air temperature set to $-15\,°C$. Wind speed was held constant at $0.6\,m/s$ for all tests. The difference in the water vapor pressure in the air and at the stone surface was varied by adjusting the temperature of the stone surface and the relative humidity in the air. The average relative humidity ranged between 58.9% and 91.4% across the different tests, and the maximum obtained difference between air temperature and stone surface temperature was $8.5\,°C$.

The stability of the different parameters and the mass accumulation during a typical frost growth test are shown in Figure 4.1. In the test shown in Figure 4.1 the average relative humidity was 59.9%, with a maximum value of 61.3% and a minimum value of 58.9%. The average air temperature was $0.7\,°C$, fluctuating between $0.6\,°C$ and $0.8\,°C$. The temperature of the stone decreased in the first minutes of the test before it stabilized at $-7.8\,°C$. The real time measured mass, m_r, showed small deviations over time compared to the manually measured mass, m_m, found by weighing the stone before and after frost growth. For this specific test m_r was 11% less than m_m. Overall, the deviation varied between -25% and +50% for the tests. This is likely to be due to the scale drifting. All hoar frost growth rates are therefore calculated based on the manually measured mass, m_m.

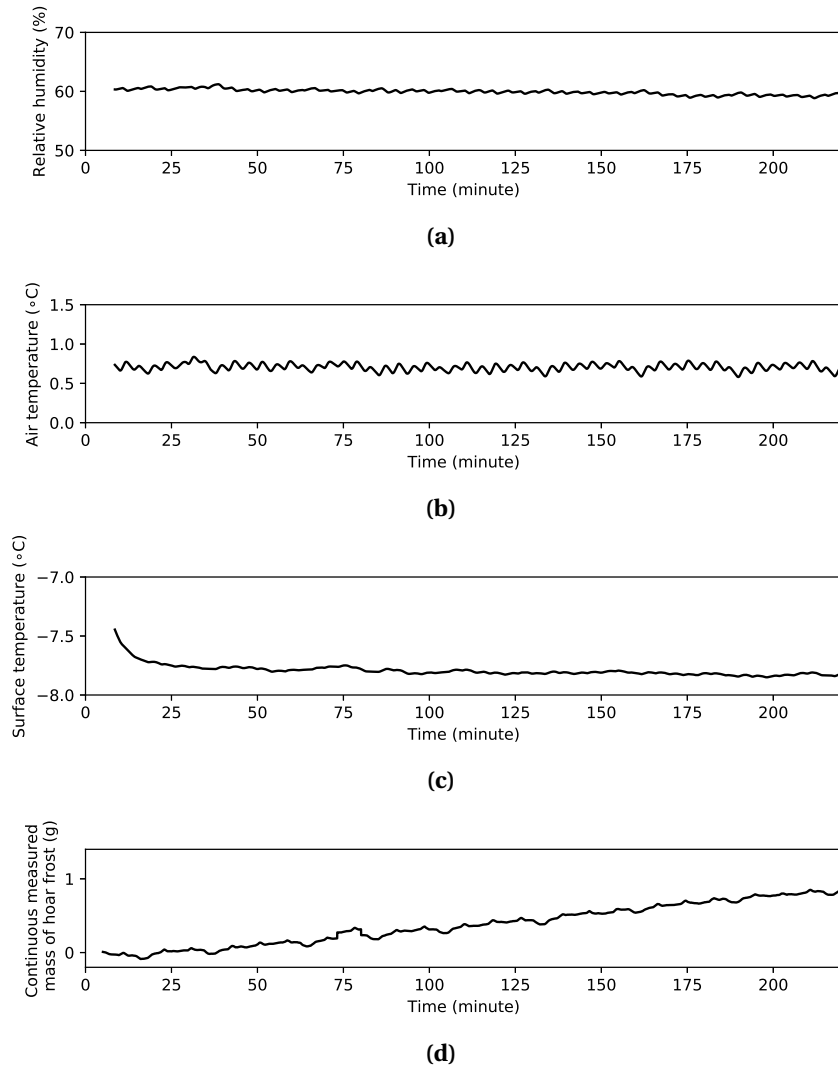**(a)**

(b)

(c)

(d)

Figure 4.1: Stability of measured parameters during test 7: (a) relative humidity, (b) air temperature, (c) surface temperature, (d) real time measured mass of hoar frost, m_r .

Figure 4.2 shows the frost growth rate, $\dot{m}$, as a function of the difference in the vapor pressure in the air and at the frost surface for all tests. The frost growth rate was found by dividing the measured mass, m_m, by the stone area and the time used for each test. $p_{v,a}$ was calculated from the measured mean values of RH and T_a and $p_{v,fs}$ was calculated from the measured mean value of T_s. Tests with air temperature $T_a = 2\,°C$ are marked with crosses and those with

$T_a = -15\,°\text{C}$ are marked with dots. A linear trend is shown and there are no distinct differences between the results from the two different air temperatures. Linear regression was used to find the mass transfer coefficient, K_p, in Eq. (2.1). $K_p = 1.35 \times 10^{-7}\,\text{kg}\,\text{m}^{-2}\,\text{s}^{-1}\,\text{Pa}^{-1}$ is valid for the setup with a wind speed of $0.6\,\text{m/s}$. This coefficient is used in Paper II where the effect of chemicals on the mass flux is investigated. Data from both temperatures were used, and the coefficient of determination, R^2, was found to be 0.99. The linear regression was forced through the origin to ensure zero hoar frost growth when the partial vapor pressure difference was zero.
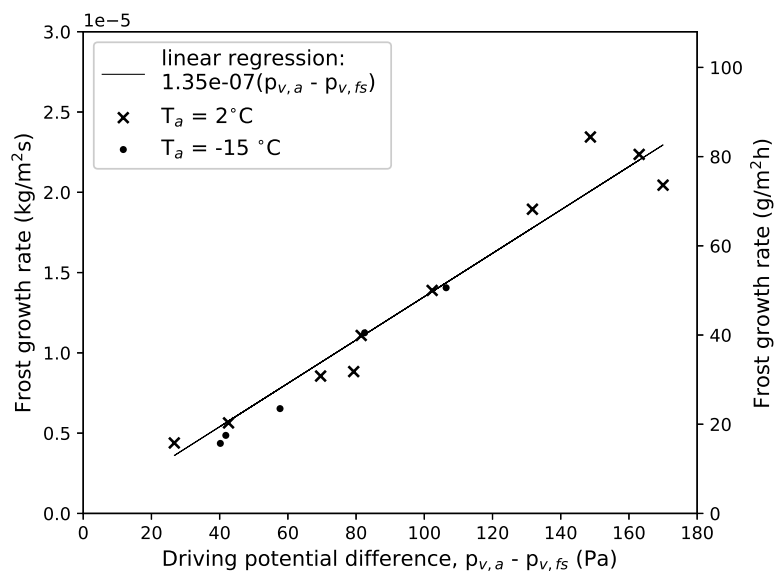

Figure 4.2: Frost growth rate as a function of the difference in the vapor pressure in the air and at the frost surface.

4.2 Direction of humidity transport - Paper IV

The direction of the transport of water between vapor and liquid is determined, as previously mentioned, by the water activity in the respective phase. In the case where RH = a_w^{sol}, liquid and vapor are in equilibrium and no net transport between a road and the air will occur. When $a_w^{sol} <$ RH, water will be transported from the vapor phase in air to a liquid solution at the surface, making the road humid. The condensation of vapor will dilute the solution on the road, increasing its water activity, until solution and vapor are in equilibrium ($a_w^{sol} =$ RH). When $a_w^{sol} >$ RH, on the other hand, water will evaporate from a wet road. When water leaves the solution on

the road, its water activity will decrease. The evaporation will continue until vapor and solution comes into equilibrium, or until all water has evaporated leaving a dry road.

In Figure 4.3, the water activity for saturated solutions of NaCl, MgCl$_2$ and CaCl$_2$ as a function of temperature is shown together with the water activity of mixes of the same chemicals. The saturated solution has the lowest possible water activity for that specific chemical at the given temperature. This figure shows that a saturated solution of NaCl has an a_w that is only slightly
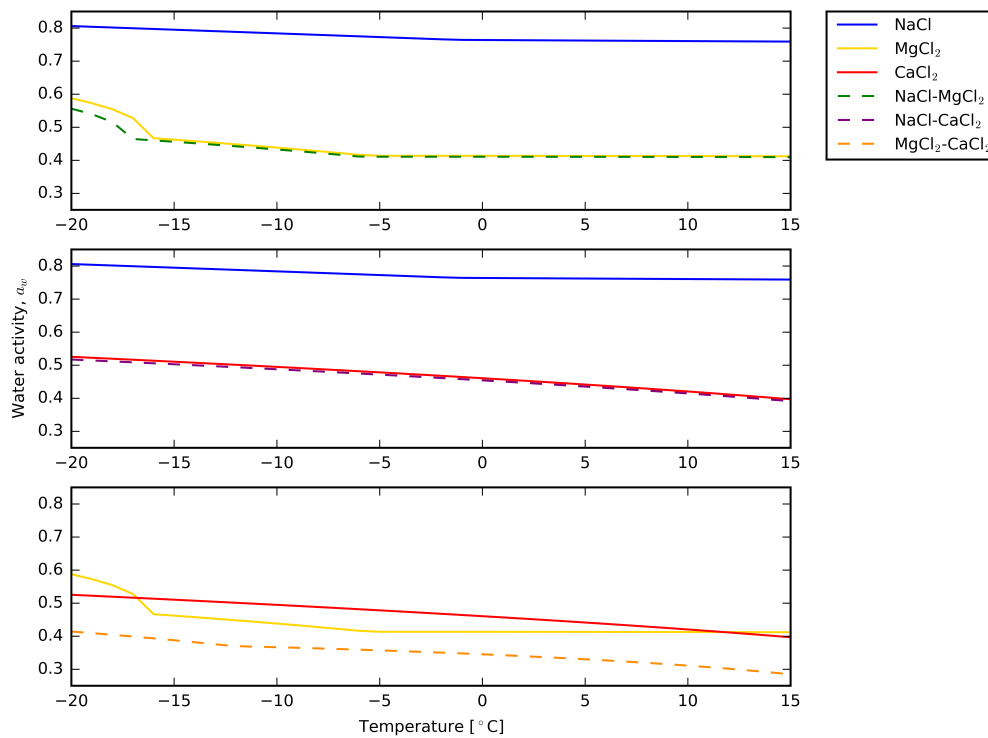

Figure 4.3: The water activity, a_w, for saturated solutions of NaCl, MgCl$_2$, CaCl$_2$ and mixtures of the same salts as a function of temperature.

varying from 0.8 to 0.75 in the temperature range between -20°C and +15°C. At 0°C a saturated solution of NaCl has a water activity of 0.76. This means that when the relative humidity in the air is above 76% at 0°C water will condensate to the solution. This addition of water will dilute the solution and the dilution continues until the activity of the diluted solution reaches the relative humidity in the air, which brings the system to equilibrium. If the relative humidity is below 76 %, water will evaporate from the solution leaving crystallized NaCl on the dry road. For a saturated solution of MgCl$_2$, the a_w is quite stable around 0.4 for temperatures above -5°C. Below -5°C, the a_w of MgCl$_2$ rises slightly towards 0.5 at -15°C, before it rises further below -15°C,

reaching 0.6 at -20°C. This means that when MgCl$_2$ is present on the road surface, the road will stay wet for relative humidities over 40% when the temperature is above -5°C. The a_w for CaCl$_2$ decreases with increasing temperatures for the temperature range studied, starting at 0.5 at -20°C and falling to 0.4 at 15°C.

As described above, Figure 4.3 therefore illustrates how the direction of the humidity transport will depend on both the type of chemical present on the road surface and the relative humidity of the air. By using the thermodynamical model the water activity can also be calculated for other concentrations and similar figures can be made.

4.3   Speed of humidity transport - Paper II

Humidity transport experiments were performed with three different solutions; 30% MgCl$_2$, 30% CaCl$_2$ and 23% NaCl. In total 22 tests were performed for the three chemicals with two different film thicknesses, 0.06 mm and 0.1 mm. The air velocity was held constant at 0.6 m/s, surface temperature was set to -5°C, air temperature was set to 2°C and relative humidity was between 80 and 95 %.

Air temperature, stone surface temperature and relative humidity were set to be similar for all experiments. However, due to slow fluctuations in the relative humidity of the walk in laboratory itself, the water vapor pressure difference between the air and the stone surface varied between the different tests. The conditions were seen to be stabile throughout each test though. Due to these variation in the conditions between the different tests, a direct comparison of the different mass addition plots were not feasible. The results were therefore normalized by calculating the relative difference between the measured mass flux and the calculated theoretical mass flux for a surface without any chemical at the given conditions. This normalized value were used as parameter for the data analysis. The theoretical mass flux without salt was found form Eq. (2.1).

Figure 4.4 shows the mean relative deviation from theoretical without salt for each chemical at the different time periods for (a) the 0.06 mm and (b) the 0.1 mm applied film thicknesses. The bars show the 95 % confidence intervals. The over all finding is that the presence of anti-icing chemical on the road surface does affect the rate of humidity transport. The presence of anti-icing chemicals increase the rate up to 30 %, but the effect decreases over time as the solution gets diluted. For NaCl and CaCl$_2$, an increased rate was only seen for the thickest applied film. The fast dilution of the thinnest films of brine might diminish the effect too fast for this experimental method.
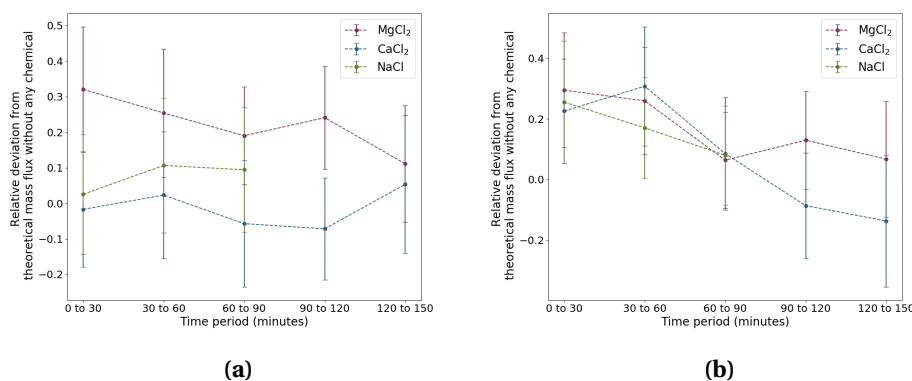
Figure 4.4: Deviation from theoretical mass flux (without any chemical) for $MgCl_2$, $CaCl_2$ and NaCl at different time periods during tests. The figure shows the mean values and the 95 % confidence intervals. (a) Film thickness of 0.06 mm. (b) Film thickness of 0.1 mm.

One-way Anova test was performed using the statsmodels module for Python to test if there was a statistically significant difference between this dataset of measured mass fluxes with salt solutions and the dataset of mass fluxes without salt from the hoar frost growth tests in section 4.1.

For the 0.06 mm thick films the presence of NaCl and $CaCl_2$ did not result in a significant increase in the mass flux for any of the time periods. For $MgCl_2$ the mass flux were seen to be significantly higher than without salt until 120-150 min, where the difference were no longer significant. For the 0.1 mm thick films all three chemicals resulted in a significant increase in the mass flux during the first 60 minutes. After 60 minutes, the difference was no longer significant for any of the tested chemicals. The differences in the mass flux between the two film thicknesses were not statistically significant for any of the three chemicals in any time period.

4.4   Hoar frost on a salted road surface - Paper III

In order to study how freezing occurs on a salted road surface occurs during hoar frost conditions, a 10% NaCl solution with freezing temperature close to the surface temperature was used. In total 18 tests with two different amounts of 10% NaCl solution were performed. For the 18 tests performed RH ranged between 78 % and 92%, T_s ranged between -4.8 °C and -6.1 °C and T_a ranged between 1.2 °C and 1.7 °C. Within each test, the RH was stable within ±2 %, T_a within ±0.2 °C and T_s within ±0.2 °C.

The formation of hoar frost on a salted surface

The formation of hoar frost was examined by visual inspections during tests and by studying photos taken every minute during the tests. Figure 4.5 shows photos taken during different stages of a test. Initially the entire surface was covered with liquid salt solution, shown in Figure 4.5(a). The freezing always started with frozen crystals floating on top of the solution, even though the system is cooled from below. Figure 4.5(b) shows this second stage where ice crystals start to appear in the salt solution. This is seen as small lines in the reflection from the light. The ice crystals continued to form on top of the solution until the entire surface was covered with ice, seen in Figure 4.5(c). By touching the frozen layer of ice with a glass plate, it was observed that liquid brine was present below the frozen layer. The start of hoar frost formation on top of the frozen layer was seen by less reflections and a more white surface. Figure 4.5(d) show an early stage of this hoar frost formation. The hoar frost dendrites continued to grow until the experiment was terminated. Figure 4.5(d) shows a distinct layer of hoar frost covering the entire surface. The further development of ice below the first observed frozen layer was not possible to study visually. However, the pendulum tests revealed that after a certain time the liquid layer disappeared and the ice adhered to the stone surface.
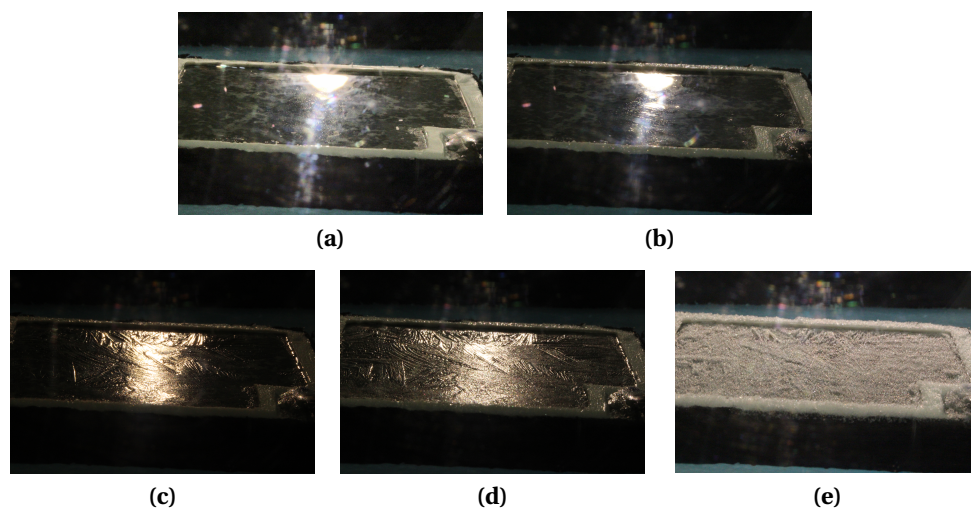

(a)　　　　　　　　　　　　(b)

(c)　　　　　　　(d)　　　　　　　(e)

Figure 4.5: Development of hoar frost formation on surface with anti-icing chemical. (a) Only liquid salt solution (b) First observable frozen crystals floating on the top of the liquid (c) Frozen crystals cover the entire surface with liquid salt solution below (d) Early stage of hoar frost formation on top of the frozen layer (e) Surface completely covered with hoar frost.

Mechanical strength of hoar frost

It was found that a significant amount of ice can be present on a salted road surface without the ice attaching to the road surface. The amount of ice removed by the pendulum were seen to depend on the amount of ice in the system of solution and ice. Figure 4.6 shows the amount of removed ice plotted against the ice fraction F_{ice} for all 18 pendulum tests. Blue dots are representing the tests with applied film thickness of 0.06 mm and black dots are representing the tests with film thickness of 0.1mm. The threshold for successful ice removal was set to more than 75 % of the ice removed. Tests with more than 75 % of the ice removed was therefore treated as "removed" and tests with less than 75 % of the ice removed was treated as "intact". Logistic regression of the tests categorized as "intact" and "removed" was performed by the use of the Scikit-learn machine learning library for Python. The probability of successful removal of the hoar frost for different ice fractions as determined by the logistic regression is also shown in Figure 4.6 for the two test series.
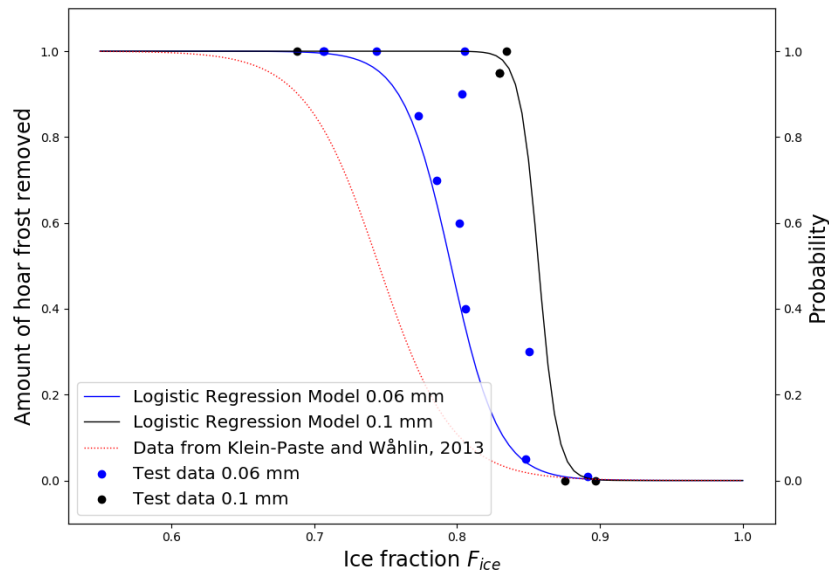

Figure 4.6: Left y-axis: Amount of hoar frost removed after five pendulum passes for the applied film thicknesses of 0.06 mm (blue dots) and 0.1 mm (black dots) for different ice fractions F_{ice}. Right y-axis: Probability of removal of hoar frost as a function of ice fraction F_{ice} for 0.06 mm applied film (blue line) and 0.1 mm applied film (black line). Dotted red line show data from Klein-Paste and Wåhlin (2013).

It is seen that by applying a thicker film of brine, a higher ice fraction is allowed for a certain probability of hoar frost removal than for a thinner film thickness. This means that a thicker film allows a larger amount of water transported from the air to the surface for each gram of NaCl applied than a thinner film, without becoming slippery.

Klein-Paste and Wåhlin (2013) have studied the mechanical strength of frozen salt solutions without any addition of humidity from the air. Their calculated probability of ice removal from laboratory tests is shown with dotted red line in Figure 4.6. It is seen that a higher ice fraction is allowed during hoar frost conditions than for freezing without humidity transport.

From the regression it was found that for the applied film thickness of 0.06 mm the 99.9 % probability of sufficient ice removal occurs at $F_{ice} = 0.67$. For a surface temperature of -5 °C, an ice fraction of 0.67 (p=0.999) corresponds to a salt concentration of 2.6 %. This occurs after an added amount of 0.84 g of moisture from the air to the test sample.

For the series of 0.1 mm applied film thickness it is seen that the 99.9 % probability of sufficient ice removal occurs at $F_{ice} = 0.81$. For a surface temperature of -5 °C, an ice fraction of 0.81 (p=0.999) corresponds to a salt concentration of 1.5 %. This occurs after an added amount of 2.80 g of moisture from the air to the test sample.

Chapter 5

Discussion

The first section of this chapter discusses the performance of the setup, this is based both on the results in Paper I and on other findings from the consecutive experiments. Section 5.2 discusses the complete process of hoar frost formation on a salted road surface. Finally, in section 5.3, it is discussed how the findings from this thesis contributes to knowledge needed to chose the type and amount of chemical needed to avoid slippery driving conditions during a hoar frost event.

5.1 Simulation of hoar frost formation

The total amount of hoar frost formed in the tests ranged from 125 to $750 \, \text{g/m}^2$ with rates ranging from 16 to $84 \, \text{g/m}^2\text{h}$. The rates are in good agreement with hoar frost rates determined in the field (Karlsson, 2001).

The stability of the key parameters such as air temperature, surface temperature and humidity is seen to be good during each test. Despite this, the dilutions tests revealed that it was hard to reproduce the same conditions for entire test series. The origin of this issue is probably the slow fluctuation in both air temperature and air humidity in the walk-in laboratory itself. In order to make the setup less vulnerable to these fluctuations several improvements could be made. Automatic regulation of the Peltier elements would allow to chose a specific surface temperature, independently of the varying air temperature in the laboratory. The other critical part is to gain control of both the humidity and the temperature of the air leaving the water bath. Automatic control of the humidity could be obtained by adding automized positioning of the lid covering the water bath, based on the measure humidity. Better control of the air temperature could be obtained by placing the whole setup at a lower laboratory temperature, and by electrical heating rise the air temperature in the wind tunnel a few degrees, using a closed-loop system. This should make it possible to keep each variable at a desired set-point. Due to time constrains these improvements could not be developed within this thesis work.

A constant frost growth rate was seen during the entire frost growth period for the initial

tests without any salt on the surface. The water vapor pressure in the air ($p_{v,a}$) was held constant during each test. The constant frost growth rate ($\dot{m}$) implies that the vapor pressure at the frost surface also remained constant. This can only be the case if the frost surface temperature remained reasonably constant, while the frost layer grows. This was confirmed by temperature measurements with an IR thermometer revealing a temperature stability on the top surface of the frost within $\pm 0.5\,$°C during a typical frost growth period.

The deviation between the real time measured mass, m_r, and the manually measured mass, m_m, was in the range of -25% and +50% between the different tests. This variation did not correlate with the difference in the temperature or the duration of the tests. We believe the key problem is related to sensor drift, as the weight can only be reset to zero at the beginning of the test. This problem turned out to be difficult to solve in an elegant manner within the given time frame. It could probably be solved by building an automated system for lifting the stone from the scale during the tests, making it possible to perform a consecutive series of weight measurements with the scale tared before each new measurement. For the examination of the dilution process, this was solved by opening the wind tunnel and and performing manual weight measurements every 10$^{\text{th}}$ minute.

The laboratory setup was found to be useful for investigating the process of hoar frost formation on a salted road surface. The ability to attract humidity to the road surface and produce specific road conditions, such as hoar frost or humid/wet road, could be valuable in the development of optical sensors for detecting the road surface conditions. Another possible area of application with an improved setup as discussed above, is research related to the use of chemicals for dust binding. The aim is then to keep the surface humid in order to prevent dry dust from becoming suspended in the air. A specific use could be to test new products with unknown thermodynamical data, in order to examine their ability to attract humidity at different temperatures and concentrations.

5.2   Hoar frost formation on a salted road surface

Humidity transport towards a salted road surface

At a temperature of -5°C the water vapor pressure above solutions of 23w% NaCl, 30w% $CaCl_2$ and 30w% $MgCl_2$ is 20%, 38% and 49% lower, respectively, than above pure water. According to Eq. (2.1), adding any chemical to the surface should increase the mass flux of water from the air to the surface. In addition, the mass flux was expected to be largest for $MgCl_2$ and smallest for NaCl. For the thickest applied films (Fig. 4.4(b)) an increased mass flux was observed for all three chemicals during the first 60 minutes. The increase was up to 30%. The effect diminished over time due to the increased water activity in the solution as it gets diluted.

No clear systematic difference between the three chemicals can be observed in Fig. 4.4(b), despite the difference in their water vapor pressure. The vapor pressure above the start solutions was lowest for $MgCl_2$ and highest for NaCl. However, the addition of water molecules on the top surface can quickly change the vapor pressure. According to Wåhlin and Klein-Paste (2017) the diffusivity for the three chemicals also differs with highest diffusivity for NaCl, a bit lower for $CaCl_2$ and lowest for $MgCl_2$. This could possibly lead a more homogeneous mixing of NaCl than $MgCl_2$, where water molecules will accumulate in the top layer where they are added. This may reduce their difference in vapor pressure for the top layer of the solution.

For the thinnest applied films (Fig. 4.4(a)), a significantly increased mass flux was only observed for $MgCl_2$. We did not find a sound explanation for this, but we assume that also NaCl and $CaCl_2$ will increase the mass flux for small application rates, but that the effect will diminish earlier due to the faster dilution of such small amounts of solution, making it hard to detect the increased mass flux with the present setup.

The rather big confidence intervals for the mass transfer rates reveal that it is challenging to perform accurate measurements of the mass transfer rates with the present setup. The wind tunnel had to be opened every time the mass was measured, disturbing the air flow. However, by statistical analysis, it was possible to detect a significantly increased humidity transport towards the salted surface for certain application rates in the early phase of the dilution process.

The freezing of a salted road surface during conditions for hoar frost formation

In the setup used, heat is extracted from below and it is expected that the stone surface is colder than the top surface of the solution film. Nevertheless, the freezing always started from the top, with liquid solution being present below the ice. This indicates that there was a concentration gradient in the brine film. This is likely because the diffusion coefficient for water vapor in air, ($\backsim$ $10^{-5} m^2/s$)(Bolz and Tuve, 1973), is five orders of magnitude larger than the diffusion coefficient for water in salt solutions, ($\backsim 10^{-10} m^2/s$) (Wåhlin and Klein-Paste, 2017). The result was an accumulation of water molecules in the top layer which lead to a higher freezing temperature in the top layer than in the bottom layer of the solution. In such situations, vehicles will not experience the road conditions very slippery because the tire will be able to break through this thin layer of ice, reaching the underlying pavement texture. The solution of anti-icing chemicals thereby continues to protect against slippery conditions even when ice starts to form on top of the solution.

After a large enough humidity transport, it was observed by the pendulum that frozen ice was stuck to the stone surface. This indicates that the diffusion of water molecules towards the colder road surface continues also after the surface is entirely covered with ice. Due to this

diffusion, the liquid layer below the ice layer continues to dilute until the freezing temperature was reached also for the solution closest to the stone surface.

Mechanical strength of hoar frost on a salted road surface

The mechanical action of the pendulum was able to remove the ice up to a certain ice fraction. After this point the diffusion of water molecules down to the salt solution had reduced the concentration sufficiently for ice to form also in the bottom of the salt solution. The ice therefore adhered to the stone surface. Successful removal of hoar frost and ice due to mechanical exposure is explained to be important for cars to obtain sufficient friction (Klein-Paste and Wåhlin, 2013). The maximum ice fraction at which the ice was removed successfully can therefore be used to calculate the amount of water allowed to be added to a salted road surface before it becomes slippery during hoar frost formation. This information is valuable in order to optimize the usage of chemicals during hoar frost formation.

It was found that by applying a thicker film of brine, a higher ice fraction was allowed for a given probability of hoar frost removal than for a thinner film thickness. This could possibly be explained by the diffusion of water in the salt solution. At a given ice fraction the liquid layer below the ice layer is thicker for higher film thicknesses. This makes the diffusion process for water molecules down to the stone surface slower for higher film thicknesses, resulting in higher allowed ice fractions until ice adhered to the surface. Using other chemicals like $MgCl_2$ and $CaCl_2$ with lover diffusivity in water (Wåhlin and Klein-Paste, 2017) could possibly extend the protection time during hoar frost formation.

The higher allowed ice fraction reported here compared to the tests by Klein-Paste and Wåhlin (2013) might be explained by the occurrence of a frozen layer with liquid solution below. Parts of the humidity transported to the system after the occurrence of this layer was kept as hoar frost on top of the ice. This hoar frost added water to the system and raised the ice fraction without actually diluting the solution below the ice layer. Using the criterion $F_{ice} = 0.6$ proposed by Klein-Paste and Wåhlin (2013) is therefore a conservative criterion during hoar frost formation.

The effect of traffic is complex and not investigated here. Applied salt solutions may be removed from the road surface either by traffic induced spray-off or by run-off do to the road topography (Lysbakken and Norem, 2008). During hoar frost situations, traffic can affect the process in different ways. Ice already formed can be crushed, ice crystals and solution can be removed by spray-off and mixing of the diluted solution can be enhanced. In total the effect of traffic is not clear. These traffic induced effects does not apply for the area outside the wheel tracks. Sufficient friction is needed also here, if a car for some reason starts to leave the wheel tracks, either intended or unintended.

5.3   Implications for use

When determining the amount and type of chemical needed to avoid slippery road conditions during a hoar frost event, knowledge about how chemicals affect the process of hoar frost formation is needed. How the results from this thesis contributes to this knowledge will be further explained in this section.

I suggest to split the process of hoar frost formation in two, the dilution process and the freezing process. The dilution process occurs from the solution is applied on the road surface until it is diluted to its freezing concentration, c_f, at the road surface temperature. The corresponding time usage is denoted as the dilution time. The freezing process occurs from the point the freezing concentration is reached until the ice formation results in slippery road conditions. The corresponding time usage is denoted as the freezing time.

When the freezing concentration is reached the activity of water in the present solution, a_w^{sol}, equals the activity of ice, a_w^{ice}, at the same temperature. This means that their water vapor pressure at the surface is the same. Therefore, the rate of humidity transported from the air to a solution at its freezing concentration should be the same as the rate of humidity transported to ice at the same temperature. Consequently, the presence of chemicals only affect the rate of the humidity transport during the dilution process.

The sum of the dilution time and the freezing time can be seen as the protection time, i.e. the time period the applied amount of chemical protects against slippery driving conditions. It should be noticed that during conditions for hoar frost formation, when $T_s < T_d$ and $T_s < 0°C$, there will always be a net flux of water towards the road surface independently on the type and amount of chemical present. Adding chemicals only increase the time it takes for ice to form and to become a potential hazard. During conditions for hoar frost formation, being able to determine the protection time for the applied chemical is therefore important for winter maintenance practitioners.

By assume a road where the three different chemical solutions can be applied at a recommended rate of $30\,\mathrm{g/m^2}$ (Norwegian Public Road Administration, 2017) calculations can be done to illustrate how the findings from Paper II and Paper III influences on the estimated protection time. The surface temperature is assumed to be -5°C and the mass flux to the road before salt is applied is assumed to be $12.5\,\mathrm{g/m^2h}$. This is the average mass flux found by Karlsson (2001), assuming one night to be 12h.

Table 5.1 shows calculated dilution and freezing times for the different solutions. The dilution times are calculated in two ways. First, by assuming no increased mass flux due to the presence of the chemicals. Secondly, it is calculated by a 30% increased mass flux throughout the entire dilution process. A 30% higher mass flux due to chemicals is probably larger than what is expected in real life, and therefor a conservative estimate.

It is seen from the table that the longest dilution time is found for MgCl$_2$ and the shortest

Table 5.1: **Calculations of dilution times and freezing times for different anti-icing solutions during a hoar frost event. The surface temperature is assumed to be -5°C. The rate of humidity transport towards the road surface prior salt application is assumed to be 12.5 g/m^{2}h. The surface temperature is assumed to be -5°C.**

Case	Applied amount of solution (g/m^2)	Applied solution	Dilution time without increased flux $F_{ice} = 0$ (h)	Dilution time with increased flux $F_{ice} = 0$ (h)	Freezing time $F_{ice} = 0.67$ (h)
1	30	23% NaCl	4.6	3.5	14.2
2	30	30% CaCl$_2$	6.5	5.0	16.6
3	30	30% MgCl$_2$	8.1	6.2	20.2

dilution time is found for NaCl, with CaCl$_2$ in between. NaCl has the shortest protection time because it cannot dissolve in much higher concentrations than 23%. The difference between MgCl$_2$ and CaCl$_2$ are due to the difference in freezing concentration at a given temperature. The amount of water added before they reach their freezing concentration therefore differs. By including the increased mass flux of 30%, the dilution time for all chemicals were reduced by approximately 20 %.

If it is assumed that the freezing temperature has to be kept below the road surface temperature, the protection time for a given application corresponds to the dilution time. The freezing time in Table 5.1 is the additional time gained when using the critical ice fraction found in Paper III, in stead of the freezing concentration criterion. When ignoring the increased mass flux during the dilution period, the total protection time for NaCl, CaCl$_2$ and MgCl$_2$ is ~19h, ~23h and ~28h, respectively. Out of this, the dilution process covers ~25% of the time and the freezing process covers ~75% of the time. When including the increased mass flux during the dilution period, the total protection time is reduced by only 5-7% of the protection time calculated without the increased mass flux.

Practically, this means that ignoring the increased mass flux towards a salted road surface, caused by the presence of chemicals, does not lead to considerable errors when estimating the protection time for an anti-icing application. However, due to the differences between different deicing chemicals in solubility and freezing concentration, the freezing times differs for the three chemicals, resulting in differences in the estimated protection times. This means that which chemical is chosen plays a large role in how long the protection time against hoar frost becomes.

As seen in Paper IV, the different chemicals might have different impact on the road surface conditions after the hoar frost situation. When applying chemicals on a road it can be desirable that the road dries up afterwards. A dry road is often preferable to avoid freezing of the solution on the road if the temperature drops, and to reduce the amount of drifting snow sticking to the

road (Perchanok et al., 1991). The road will dry up if the relative humidity in the air (in fraction, not %) is below the water activity of the saturated solution at the given temperature. At -5℃ a solution of NaCl will dry up for RH < 78%, while for $CaCl_2$ and $MgCl_2$ a relative humidity below 48% and 41% is needed for the road to dry up. With that in mind, it can be beneficial to chose a chemical with a shorter protection time which gives a road that dries up faster and becomes easier to maintain over time. On the other hand, salt is also used for dust binding. The aim in dust binding is to keep the road surface humid in order to prevent dry dust from becoming suspended in the air. Then, $MgCl_2$ and $CaCl_2$ is the preferable chemicals.

Chapter 6

Conclusions and further work

6.1 Conclusions

The following main conclusions can be draw from the presented work:

- A setup simulating hoar frost formation when warm, humid air flows over a cold road surface has been developed. The setup has proven sufficient stability of critical parameters during tests, and the resulting hoar frost growth rates were in the range of those earlier reported on-site.

- The direction of the humidity transport between the air and solutions of NaCl, $CaCl_2$, $MgCl_2$, can be found by comparing the water activity for the solution and the relative humidity of the air. The water activity can be found for different concentrations, mixes and temperatures from a thermodynamical model, such as the Extended UNIQUAC model.

- If the water activity for the solution is lower than the relative humidity in the air, humidity is transported to the solution. If the water activity of the solution is higher than the relative humidity in the air, humidity is transported to the air.

  In order for the road to dry up, the relative humidity in the air has to be below the water activity for the saturated concentration of the solution. Opposite, if the aim is to keep the road humid/wet, the criterion is that the water activity for the saturated concentration of the solution is below the the relative humidity in the air.

- The presence of anti-icing chemicals does increase the mass flux towards the surface for certain application rates. The effect was up to 30 % and significant for both NaCl, $CaCl_2$ and $MgCl_2$ for a film thickness of 0.1 mm. For a film thickness of 0.06 mm the effect was only significant for $MgCl_2$. The effect was seen to diminish during the first two hours as the solution was diluted.

- For the investigated hoar frost conditions the solution was seen to freeze from top, even though the top was warmer than the solution/stone interface. This indicates that there is a concentration gradient in the solution due to slower diffusion of water in the salt solution than in the air.

- The freezing process can continue up to a given ice fraction, before the formed ice is so strong that simulated traffic cannot remove the ice. A higher ice fraction was acceptable for higher applications rates. For a film thickness of 0.06 mm a critical ice fraction of 0.67 was found, while for a film thickness for 0.1 mm a critical ice fraction of 0.81 was found.

- The protection time for an anti-icing action during conditions for hoar frost formation is strongly underestimated when defining the end of the protection time to when the first ice crystals form in the solution. Since we, in reality can accept much more ice on the road, significantly less chemicals can be used.

- When ignoring the increased mass flux caused by the presence of anti-icing chemicals during the dilution period, the dilution time covers ~25% and the freezing time ~75% of the total protection time. When including the increased mass flux during the dilution period, the total protection time is reduced by only 5-7% of the protection time calculated without the increased mass flux.

- The main difference in protection time between different chemicals is a consequence of the differences in their solubility and the amount of water that can be added prior the solution is diluted to its freezing concentration, not in their ability to attract humidity from the air.

6.2 Further work

- Freezing was observed to start in the top layer of the solution during hoar frost conditions. The slow diffusion of water molecules in the salt solution is expected to be the origin for this. Therefore, it would be of interest to investigate the critical ice fraction for other solutions, such as $MgCl_2$ and $CaCl_2$, with lower diffusivity than NaCl.

- Work should be done in order to implement the improvements discussed in section 5.2 to the setup. This includes both the ability to perform real time weight measurements of the slowly changing mass, and the ability to chose climatic parameters independently of the slow fluctuations in the climate of the walk-in laboratory itself.

- The effect of traffic to both the dilution process and the freezing process should be investigated and used to further improve the estimated protection times.

Bibliography

Andersson, A. and Chapman, L. (2011). The use of a temporal analogue to predict future traffic accidents and winter road conditions in Sweden. *Meteorological Applications*, 18(2):125–136.

Atkins, P. and Paula, J. D. (2006). *Physical Chemistry*. Oxford University Press, 9th edition.

Bolz, R. E. and Tuve, G. L., editors (1973). *CRC Handbook of Tables for Applied Engineering Science*. CRC Press, 2nd edition.

Cargill, Incorporated. *SafeLine HDX Sell Sheet. https://www.cargill.com/doc/1432076037079/sl-hdx-sell-sheet.pdf. January 2020*.

Cheng, Chin-Hsiang; Wu, K.-H. (2003). Observations of early-stage frost formation on a cold plate in atmospheric air flow. *Journal of Heat Transfer*, 125:95–102.

Crevier, L.-P. and Delage, Y. (2001). Metro: A new model for road-condition forecasting in Canada. *Journal of Applied Meteorology*, 40(11):2026–2037.

Dave, E. V., Kostick, R. D., and Dailey, J. (2017). Performance of high friction bridge deck overlays in crash reduction. *Journal of Performance of Constructed Facilities*, 31(2):04016094.

Denby, B. R., Sundvor, I., Johansson, C., Pirjola, L., Ketzel, M., Norman, M., Kupiainen, K., Gustafsson, M., Blomqvist, G., Kauhaniemi, M., and Omstedt, G. (2013). A coupled road dust and surface moisture model to predict non-exhaust road traffic induced particle emissions (NORTRIP). Part 2: Surface moisture and salt impact modelling. *Atmospheric Environment*, 81:485–503.

Evans, J. F. (2010). Evaluation of the SafeLane™ overlay system for crash reduction on bridge deck surfaces. Technical Report MN/RC 2010-13, Minnesota Department of Transportation Research Services Section.

Fay, L. and Shi, X. (2012). Environmental impacts of chemicals for snow and ice control: State of the knowledge. *Water, Air, & Soil Pollution*, 223(5):2751–2770.

Friar, S. and Decker, R. (1999). Evaluation of a fixed anti-icing spray system. *Transportation Research Record*, 1672(1):34–41.

Fujimoto, A., Tokunaga, R., Kiriishi, M., Kawabata, Y., Takahashi, N., Ishida, T., and Fukuhara, T. (2014). A road surface freezing model using heat, water and salt balance and its validation by field experiments. *Cold Regions Science and Technology*, 106–107:1–10.

Giles, C. G., Sabey, B. E., and Cardew, K. H. F. (1964). Development and performance of the portable skid-resistance tester. Technical Report 66, Road Research Laboratory, London.

Greenfield, T. M. and Takle, E. S. (2006). Bridge frost prediction by heat and mass transfer methods. *Journal of Applied Meteorology and Climatology*, 45(3):517–525.

Haavasoja, T., Nylander, J., and Nylander, P. (2012). Relation of road surface friction and salt concentration. In *Proceedings of the 16th SIRWEC conference 23–25th may 2012*.

Hanson, R., Klashinsky, R., Day, E., and Cottone, B. (2013). Evaluating automated anti-icing technology to reduce traffic collisions. *Presented at 2013 Conference of the Transportation Association of Canada, Winnipeg, Manitoba, Sept. 22–25, 2013*.

Hermes, C. J., Piucco, R. O., Barbosa Jr., J. R., and Melo, C. (2009). A study of frost growth and densification on flat surfaces. *Experimental Thermal and Fluid Science*, 33(2):371–379.

Job, G. and Herrmann, F. (2006). Chemical potential - a quantity in search of recognition. *European journal of physics*, 27:353–371.

Johnsson, J. (2017). *Winter Road Maintenance using Renewable Thermal Energy*. PhD thesis, Chalmers University of Technology.

Kandula, M. (2011). Frost growth and densification in laminar flow over flat surfaces. *International Journal of Heat and Mass Transfer*, 54(15–16):3719–3731.

Kandula, M. (2012). Frost growth and densification on a flat surface in laminar flow with variable humidity. *International Communications in Heat and Mass Transfer*, 39(8):1030 – 1034.

Karlsson, M. (2001). Prediction of hoar-frost by use of a road weather information system. *Meteorological Applications*, 8(01):95–105.

Ketcham, S. A., Minsk, L. D., Blackburn, R. R., and Fleege, E. J. (1996). Manual of practice for an effective anti-icing program: A guide for highway winter maintenance personnel. Technical Report 2/22/96, US Army Cold Regions Research and Engineering Laboratory.

Klein-Paste, A. and Wåhlin, J. (2013). Wet pavement anti-icing - a physical mechanism. *Cold Regions Science and Technology*, 96:1 – 7.

Knollhoff, D. S., Takle, E., Gallus, W., Burkheimer, D., and McCauley, D. (2003). Evaluation of a frost accumulation model. *Meteorological Applications*, 10(4):337–343.

Knollhoff, D. S., Takle, E. S., Gallus Jr, W. A., and Burkheimer, D. (1998). Use of pavement temperature measurements for winter maintenance decisions. In *Transportation Conference Proceedings*, pages 33–36.

Koop, T., Luo, B., Tsias, A., and Peter, T. (2000). Water activity as the determinant for homogeneous ice nucleation in aqueous solutions. *Nature*, 406(6796):611–614.

Li, Y., Fang, Y., Seeley, N., Jungwirth, S., Jackson, E., and Shi, X. (2013). Corrosion by chloride deicers on highway maintenance equipment: Renewed perspective and laboratory investigation. *Transportation Research Record*, 2361(1):106–113.

Lysbakken, K. R. and Norem, H. (2008). The amount of salt on road surfaces after salt application. In *Transportation Research Circular E-C126: Surface Transportation Weather and Snow Removal and Ice Control Technology*, pages 85–101, Washington, D.C. Transportation Research Board of the National Academies.

Minsk, L. D. (1998). *Snow and Ice Control Manual for Transportation Facilities*. McGraw-Hill.

Murphy, D. M. and Koop, T. (2005). Review of the vapour pressures of ice and supercooled water for atmospheric applications. *Quarterly Journal of the Royal Meteorological Society*, 131(608):1539–1565.

Na, B. and Webb, R. L. (2004). New model for frost growth rate. *International Journal of Heat and Mass Transfer*, 47(5):925–936.

Norrman, J., Eriksson, M., and Lindqvist, S. (2000). Relationships between road slipperiness, traffic accident risk and winter road maintenance activity. *Climate Research*, 15:185–193.

Norwegian Public Road Administration (2017). *Usage of salt (in norwegian)*, D2-ID9300a-7 edition.

Ou, T., Hu, Y., Gustavsson, T., and Bogren, J. (2019). On the relationship between the risk of hoar frost on roads and a changing climate in Sweden. *International Journal of Climatology*, 39(5):2601–2611.

Perchanok, M., Manning, D., and Armstrong, J. (1991). Highway de-icers: Standards, practices and research in the province of Ontario.

POLY-CARB. *Proven Performance Systems. https://olinpolycarb.com/applications/bridge-deck-overlay/. January 2020.*

Rämä, P. (1999). Effects of weather-controlled variable speed limits and warning signs on driver behavior. *Transportation Research Record*, 1689(1):53–59.

Rämä, P. and Luoma, J. (1997). Driver acceptance of weather-controlled road signs and displays. *Transportation Research Record*, 1573(1):72–75.

Ramakrishna, D. M. and Viraraghavan, T. (2005). Environmental impact of chemical deicers – A review. *Water, Air, and Soil Pollution*, 166(1):49–63.

Sass, B. H. (1992). A numerical model for prediction of road temperature and ice. *Journal of Applied Meteorology*, 31(12):1499–1506.

Shi, X., Jungwirth, S., Akin, M., Wright, R., Fay, L., Veneziano, D., Zhang, Y., Gong, J., and Ye, Z. (2014). Evaluating snow and ice control chemicals for environmentally sustainable highway maintenance operations. *Journal of Transportation Engineering*.

SHT (2010). Rapport om møteulykke mellom vogndtog og to personbiler på E16 i Flåm 16. november 2007. Technical report, Statens Havarikommisjon for Transport (SHT).

Stanton, B., Miller, D., and Adams, E. (2012). Analysis of surface hoar growth under simulated meteorological conditions. In *Proceedings, 2012 International Snow Science Workshop, Anchorage, Alaska*.

Thomsen, K. (2005). Modeling electrolyte solutions with the extended universal quasichemical (uniquac) model. *Pure and Applied Chemistry*, 77:531–542.

Veneziano, D., Ye, Z., and Turnbull, I. (2014). Speed impacts of an icy curve warning system. *IET Intelligent Transport Systems*, 8(2):93–101.

Wåhlin, J. and Klein-Paste, A. (2017). The effect of mass diffusion on the rate of chemical ice melting using aqueous solutions. *Cold Regions Science and Technology*, 139:11 – 21.

Webb, R. L. (1990). Standard nomenclature for mass transfer processes. *International Communications in Heat and Mass Transfer*, 17(5):529–535.

Xu, G. and Shi, X. (2018). Impact of chemical deicers on roadways infrastructure: Risks and best management practices. In Shi, X. and Fu, L., editors, *Sustainable winter road operations*. John Wiley & Sons.

Zhang, J., Das, D., and Peterson, R. (2009). Selection of effective and efficient snow removal and ice control technologies for cold-region bridges. *Journal of Civil, Environmental, and Architectural Engineering*, 3(1):1–14.

Paper I
Experimental setup simulating hoar frost formation on roadways

Fjærestad, J. S., Wåhlin, J. and Klein-Paste, A. (2020). Journal of Cold Regions Engineering

Experimental Setup Simulating Hoarfrost Formation on Roadways

Janne Siren Fjærestad[1], Johan Wåhlin[2], and Alex Klein-Paste[3]

[1]Department of Civil and Transport Engineering, Norwegian University of Science and

Technology, NO-7491, Trondheim, Norway. Email: janne.fjarestad@ntnu.no

[2]Norwegian Public Roads Administration, Abels gate 5, NO-7030, Trondheim, Norway

[3]Department of Civil and Transport Engineering, Norwegian University of Science and

Technology, NO-7491, Trondheim, Norway

ABSTRACT

Hoarfrost on roadways and bridges can cause slippery and dangerous conditions for motorists. To reduce the costs and environmental impacts of countermeasures the road authorities wish to optimize their winter maintenance operations. To support this, good knowledge of the hoarfrost formation process is needed. This paper presents a laboratory setup designed and built to study hoarfrost formation in detail under controlled conditions. The accumulation of hoarfrost (g/m^2) and the stability of the main controlling parameters (air temperature, surface temperature and relative humidity) are quantified. By using an open loop wind tunnel with warm, humid air flowing over a cold stone surface, we produced conditions similar to those of frost formation on a road with good stability. The hoarfrost growth rates were found to be within the range of field measurements earlier published. The growth rates were constant during each test and were directly related to the driving force created by the difference in the water vapor pressure in the air and at the stone surface.

INTRODUCTION

Hoarfrost on roadways and bridge decks can cause slippery and dangerous conditions for motorists, especially at the beginning of the winter season (Norrman et al. 2000). In Sweden in the

winters of 2004-2005 and 2005-2006, 18.1% and 14.5% of accidents respectively occurred during hoarfrost formation (Andersson and Chapman 2011).

Different actions can be taken to reduce the risk of accidents due to hoarfrost, for example use of friction overlays (Evans 2010; Dave et al. 2017), monitoring road surface conditions (Minsk 1998), heating the road surface (Minsk 1999) and the application of freezing-point depressant chemicals (Ketcham et al. 1996). Due to their negative economic and environmental impacts (Ramakrishna and Viraraghavan 2005; Fay and Shi 2012) it is desirable to optimize the use of heating and chemicals. A key to this is good prediction of hoarfrost formation, both its duration and severity.

A number of models for predicting surface temperature and surface state (e.g. dry, wet, snowy, icy) on both roads and bridge decks already exist (e.g. Sass 1992; Crevier and Delage 2001; Knollhoff et al. 2003; Greenfield and Takle 2006; Denby et al. 2013 and Fujimoto et al. 2014). These models can predict when the conditions for hoarfrost formation is present. But, to the best of our knowledge, little is known about when deposited hoarfrost actually leads to slippery conditions. Since chemicals (for example sodium chloride) are frequently used during these events, it is also of interest how and how long these chemicals prevent the hoarfrost growth process. Being able to simulate hoarfrost growth in a laboratory setup will make it possible to gain further understanding of these issues when systematically adjusting the main controlling parameters of hoarfrost formation.

Several researchers have developed experimental setups for hoarfrost formation earlier. Stanton et al. (2012) used a cold ceiling to simulate long wave radiation loss due to clear sky conditions. Cheng (2003), Hermes et al. (2009) and Kandula (2011) simulated hoarfrost formation with warm humid air flowing over a cold surface. Common for these experiments is that they produced hoarfrost at much higher rates than realistic for road situations. The air temperatures were typically between 15 to 25 °C, and the frost surface temperatures were between −5 to −20 °C.

In order to study the hoarfrost formation on road surfaces in detail, we developed an experimental setup that can simulate hoarfrost formation at deposition rates that are more realistic than previous experimental setups. Similar to Cheng (2003), Hermes et al. (2009) and Kandula (2011), we extracted heat from the bottom of the surface downwards, simulating the conditions of warm humid

air passing over a colder road surface. The experiment proved that this setup demonstrates sufficient stability of the key parameters and that it is possible to adjust these within a range of values relevant to winter roads.

METHOD

Theory

Hoarfrost occurs when water vapor in the air changes from a gaseous state to a solid state on a cold surface. This can occur when the surface temperature is lower than both the dew point and the temperature at which water freezes. The mechanism behind this mass transport is the difference in the energy state for water molecules in the air and at the frost surface. Water molecules will prefer the state with the lowest energy. The rate of the resulting hoarfrost growth rate can be described using different driving potentials, for example partial pressure, molar density, and mass density (Webb 1990). Using the partial pressure of water vapor as the driving potential, the rate of the resulting frost growth can be described as:

$$\dot{m} = K_p(p_{v,a} - p_{v,fs}) \tag{1}$$

where K_p is the mass transfer coefficient, $p_{v,a}$ is the water vapor pressure in the air flow and $p_{v,fs}$ is the water vapor pressure at the frost surface.

The water vapor pressure in the air, $p_{v,a}$, is calculated from the definition of the relative humidity:

$$RH = \frac{p_{v,a}}{p_{v,a}^{sat}} \cdot 100 \tag{2}$$

where RH is the measured relative humidity and $p_{v,a}^{sat}$ is saturation vapor pressure at the given air temperature, T_a.

Air is assumed to be saturated at the frost surface (Kandula 2011). The water vapor pressure at the frost surface, $p_{v,fs}$, is therefore given as the saturation vapor pressure at the surface temperature, T_s.

Hoarfrost growth

A setup as shown in Fig. 1 was build inside a walk-in cold temperature laboratory. The setup was designed to simulate typical conditions for frost formation on road surfaces, with air velocities ranging from 0.6 m/s to 1.2 m/s, relative humidity from 60% to 100%, air temperatures from −20 °C to 5 °C, and surface temperatures ranging from air temperature to 8 °C below air temperature.

The setup was designed as an open loop wind tunnel in which humid air flowed over a cold stone surface, see sketch in Fig. 2. The air flow was driven by tangential fan 1 placed at the end of the loop. The wind speed, v, was measured at a location 1.5 cm above the stone surface using a Fluke 975V AirMeter (sensor 3) and controlled by adjusting the fan voltage. Water vapor was added to the air by placing a water bath in front of the stone surface. The amount of vapor added could be controlled by adjusting the water temperature and the open area of the water bath, using an adjustable lid. During tests it was found to be easier to adjust the lid than the bath temperature. A bath temperature of 25 °C was used for the tests presented here. The build-up of hoarfrost took place on an 80 mm x 80 mm stone with a height of 9 mm. Typical asphalt concrete consists of 95% stone and 5% mastic, which is bitumen and filler. Therefore, it was decided to use a stone in order to achieve an even heat transfer through the test sample and to avoid potential artifacts due to the presence of mastic. The stone was cooled by 4 Peltier elements connected in series. The cooling of the Peltier elements took place in a separate wind loop below the humidity transport loop. The two loops were separated by a 5 cm thick layer of XPS insulation placed around the stone. The Peltier elements were placed on a pin fin heat sink, and an additional fan (fan 2 in Fig. 2) was added below the insulation to improve the heat convection from the warm side of the Peltier elements. The stone surface temperature was controlled by adjusting the voltage on the Peltier elements.

The different parameters measured during the experiments are listed in Table 1. The real-time amount of hoarfrost deposited on the stone surface, m_r, was logged using an electronic scale during frost formation. To control this real time measurement of the mass, the stone was also removed from the setup and weighed on another electronic scale before and after each frost growth test. This manually measured mass difference between the start and end of each test was denoted m_m.

The relative humidity, RH, was measured using a Vaisala HMT337 sensor with a warmed probe allowing measurements up to 100% RH. The humidity sensor was calibrated at 2 °C by an HMK15 calibration kit, using NaCl as reference.

The air temperature inside the setup, T_a, was measured with a temperature probe integrated in the Vaisala HMT337 sensor. Humidity and air temperature were measured 9 cm in front of the stone at a height of 2.5 cm above the stone surface (sensor 1 in Fig. 2). The surface temperature of the stone, T_s, was measured using a Pt100 glued at a corner of the stone (sensor 2). The temperature sensors were calibrated in a slush of finely crushed ice and water.

RESULTS

In total 15 frost growth tests were performed. Ten were performed with an air temperature of 2 °C, and five with an air temperature set to −15 °C. These two test series are referred to as performed at $T_a = 2$ °C and $T_a = -15$ °C, even though the measured T_a varied between the different tests. Wind speed was held constant at 0.6 m/s for all tests. The difference in the water vapor pressure in the air and at the stone surface was varied by adjusting the temperature of the stone surface and the relative humidity in the air. The average relative humidity ranged between 58.9% and 91.4% across the different tests, and the maximum obtained difference between air temperature and stone surface temperature was 8.5 °C.

An overview of the measured and calculated parameters and their standard deviations, is found in Table 2. Data were sampled at a frequency of 2.4 Hz and filtered over 1000 measurements, i.e. 6.9 minutes, using a rolling mean filter. Analysis was performed from the point when the surface temperature dropped below the dew point. The stability of the different parameters and the mass accumulation during a typical frost growth test are shown in Fig. 3. In the test shown i Fig. 3 the average relative humidity was 59.9%, with a maximum value of 61.3% and a minimum value of 58.9%. The average air temperature was 0.7 °C, fluctuating between 0.6 °C and 0.8 °C. The temperature of the stone decreased in the first minutes of the test before it stabilized at −7.8 °C.

The real time measured mass, m_r, showed small deviations over time compared to the manually measured mass, m_m, found by weighing the stone before and after frost growth. This is likely to be

due to the scale drifting. All hoarfrost growth rates are therefore calculated based on the manually measured mass, m_m.

Fig. 4 shows (a) the stone without hoarfrost, (b) typical frost growth after tests performed at $T_a = 2\,°C$ and (c) at $T_a = -15\,°C$. The frost pattern is homogenous in both images, indicating that the surface temperature of the stone is homogeneous. At $2\,°C$ the frost structure is dense, while at $-15\,°C$ there is a coarser frost structure with more air between each crystal.

Fig. 5 shows the frost growth rate, $\dot{m}$, as a function of the difference in the vapor pressure in the air and at the frost surface for all tests. The frost growth rate was found as the measured mass, m_m, divided by the stone area and the time used for each test. $p_{v,a}$ was calculated from the measured mean values of RH and T_a and $p_{v,fs}$ was calculated from the measured mean value of T_s. Tests with air temperature $T_a = 2\,°C$ are marked with crosses and those with $T_a = -15\,°C$ are marked with dots. A linear trend is shown and there are no distinct differences between the results from the two different air temperatures. Linear regression was used to find the mass transfer coefficient, K_p, in Eq. (1). $K_p = 1.35 \times 10^{-7}\,\mathrm{kg\,m^{-2}\,s^{-1}\,Pa^{-1}}$ is valid for the setup with a wind speed of $0.6\,\mathrm{m/s}$. Data from both temperatures were used, and the coefficient of determination, R^2, was found to be 0.99. The linear regression was forced through the origin to ensure zero hoarfrost growth when the partial vapor pressure difference was zero.

DISCUSSION

The total amount of hoarfrost formed in the tests ranged from 125 to $750\,\mathrm{g/m^2}$ with rates ranging from 16 to $84\,\mathrm{g/m^2h}$. Karlsson (2001) reports amounts of hoarfrost deposited during one night in the range of 55 to $495\,\mathrm{g/m^2}$. The rates are not given, but by assuming 12 h of frost growth during each test it can be estimated that they are in the range of 5 to $41\,\mathrm{g/m^2h}$. If any sublimation occurred during this period, the real rates are higher. Both the total amount of hoarfrost and the rates from the laboratory setup are thus realistic.

The stability of the key parameters such as air temperature, surface temperature and humidity is seen as sufficient for the purpose during the tests. As shown in Fig. 3 (d) a constant frost growth rate was seen during the entire frost growth period in our test. The same linear growth was seen in

all tests. The water vapor pressure in the air ($p_{v,a}$) was held constant during the tests. The constant frost growth rate ($\dot{m}$) implies that the vapor pressure at the frost surface also remained constant. This can only be the case if the frost surface temperature remained reasonably constant, while the frost layer grows. This was confirmed by temperature measurements with an IR thermometer revealing a temperature stability on the top surface of the frost within $\pm 0.5\,°C$ during a typical frost growth period. It can therefore be argued that the cooling of the frost surface is not limited by the transport of heat through the frost layer for the amounts of hoarfrost ($125 - 750\text{g/m}^2$) and the temperature conditions ($T_a - T_s < 9\,°C$) studied here. Despite the constant growth rate in all the test runs, the deviation between m_r and m_m varied between the different tests. This variation did not correlate with the difference in the temperature or the duration of the tests. We believe the key problem is related sensor drift, as the sensor can only be reset to zero at the beginning of the test. This problem could be solved by building an automated system for lifting the stone from the scale during the tests, making it possible to perform a consecutive series of weight measurements with the scale tared before each measurement. It would also be possible to determine the mass development of the hoarfrost throughout the tests by performing manual weight measurements at specific time intervals.

The ability to produce and measure realistic amounts of hoarfrost under realistic road surface conditions is valuable for further understanding the following issues:

- how different amounts or types of hoarfrost affects the road surface friction
- how the hoarfrost formation process is influenced by the presence of salt
- the dilution rate of applied anti-icing agents

All these phenomena are important when optimizing the use of measures to avoid slippery roads due to hoarfrost formation, for both deciding when to use them and for estimating their duration.

CONCLUSION

A setup specifically made to study hoarfrost under conditions relevant to winter road maintenance was designed and built. By using an open loop wind tunnel with warm, humid air flowing

over a cold stone surface we were able to produce conditions similar to those of frost formation on a road with good stability. The hoarfrost growth rates were found to be within the range of field measurements earlier published. This makes the setup suitable for studying issues related to hoarfrost formation on roads such as friction and salting dosage.

The hoarfrost growth rate was found to be constant during the frost growth tests, irrespective of the thickness of the hoarfrost layer. This indicates that the frost surface temperature was stable throughout each test for the amounts of frost $(125 - 750 \mathrm{g/m}^2)$ and temperatures $(T_a - T_s < 9\,°\mathrm{C})$ studied here.

DATA AVAILABILITY STATEMENT

Data generated in the laboratory experiment and calculated data used in presented figures are available from the corresponding author by request.

REFERENCES

Andersson, A. and Chapman, L. (2011). "The use of a temporal analogue to predict future traffic accidents and winter road conditions in Sweden." *Meteorological Applications*, 18(2), 125–136.

Cheng, Chin-Hsiang; Wu, K.-H. (2003). "Observations of early-stage frost formation on a cold plate in atmospheric air flow." *Journal of Heat Transfer*, 125, 95–102.

Crevier, L.-P. and Delage, Y. (2001). "Metro: A new model for road-condition forecasting in Canada." *Journal of Applied Meteorology*, 40(11), 2026–2037.

Dave, E. V., Kostick, R. D., and Dailey, J. (2017). "Performance of high friction bridge deck overlays in crash reduction." *Journal of Performance of Constructed Facilities*, 31(2), 04016094.

Denby, B. R., Sundvor, I., Johansson, C., Pirjola, L., Ketzel, M., Norman, M., Kupiainen, K., Gustafsson, M., Blomqvist, G., Kauhaniemi, M., and Omstedt, G. (2013). "A coupled road dust and surface moisture model to predict non-exhaust road traffic induced particle emissions (NORTRIP). Part 2: Surface moisture and salt impact modelling." *Atmospheric Environment*, 81, 485–503.

Evans, J. F. (2010). "Evaluation of the SafeLane™ overlay system for crash reduction on bridge deck surfaces." *Report No. MN/RC 2010-13*, Minnesota Department of Transportation Research Services Section.

Fay, L. and Shi, X. (2012). "Environmental impacts of chemicals for snow and ice control: State of the knowledge." *Water, Air, & Soil Pollution*, 223(5), 2751–2770.

Fujimoto, A., Tokunaga, R., Kiriishi, M., Kawabata, Y., Takahashi, N., Ishida, T., and Fukuhara, T. (2014). "A road surface freezing model using heat, water and salt balance and its validation by field experiments." *Cold Regions Science and Technology*, 106–107, 1–10.

Greenfield, T. M. and Takle, E. S. (2006). "Bridge frost prediction by heat and mass transfer methods." *Journal of Applied Meteorology and Climatology*, 45(3), 517–525.

Hermes, C. J., Piucco, R. O., Barbosa Jr., J. R., and Melo, C. (2009). "A study of frost growth and densification on flat surfaces." *Experimental Thermal and Fluid Science*, 33(2), 371–379.

Kandula, M. (2011). "Frost growth and densification in laminar flow over flat surfaces." *International Journal of Heat and Mass Transfer*, 54(15–16), 3719–3731.

Karlsson, M. (2001). "Prediction of hoar-frost by use of a road weather information system." *Meteorological Applications*, 8(01), 95–105.

Ketcham, S. A., Minsk, L. D., Blackburn, R. R., and Fleege, E. J. (1996). "Manual of practice for an effective anti-icing program: A guide for highway winter maintenance personnel." *Report No. 2/22/96*, US Army Cold Regions Research and Engineering Laboratory.

Knollhoff, D. S., Takle, E., Gallus, W., Burkheimer, D., and McCauley, D. (2003). "Evaluation of a frost accumulation model." *Meteorological Applications*, 10(4), 337–343.

Minsk, L. D. (1998). *Snow and Ice Control Manual for Transportation Facilities*. McGraw-Hill.

Minsk, L. D. (1999). "Heated bridge technology." *Report No. FHWA-RD-99-158*, U.S Department of Transportation, Federal Highway Administration.

Norrman, J., Eriksson, M., and Lindqvist, S. (2000). "Relationships between road slipperiness, traffic accident risk and winter road maintenance activity." *Climate Research*, 15, 185–193.

Ramakrishna, D. M. and Viraraghavan, T. (2005). "Environmental impact of chemical deicers – A review." *Water, Air, and Soil Pollution*, 166(1), 49–63.

Sass, B. H. (1992). "A numerical model for prediction of road temperature and ice." *Journal of Applied Meteorology*, 31(12), 1499–1506.

Stanton, B., Miller, D., and Adams, E. (2012). "Analysis of surface hoar growth under simulated meteorological conditions." *Proceedings, 2012 International Snow Science Workshop, Anchorage, Alaska*.

Webb, R. L. (1990). "Standard nomenclature for mass transfer processes." *International Communications in Heat and Mass Transfer*, 17(5), 529–535.

List of Tables

TABLE 1. Overview of measured parameters

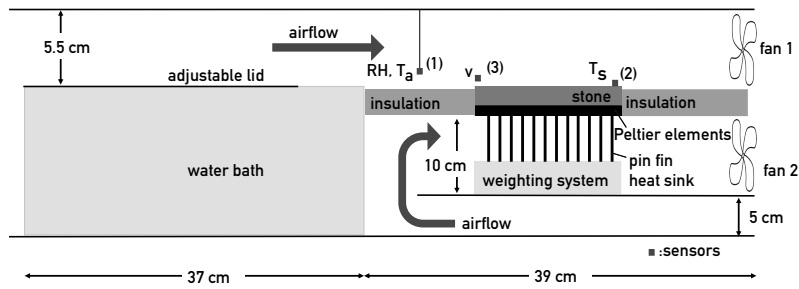| Parameter	Symbol	Unit	Instrument
Humidity	RH	%	Vaisala HMT337
Air temperature	T_a	°C	Vaisala HMT337
Surface temperature	T_s	°C	Pt100
Air velocity	v	m/s	FLUKE 975V
Mass of hoarfrost from real time measurements	m_r	g	OHAUS Pioneer PA2202
Mass of hoarfrost from manual measurement	m_m	g	AND EK-400H

TABLE 2. Overview of measured and calculated parameters from all tests

| Test #	Test duration (h)	Accumulated hoar frost (g/m^2)	Frost growth rate (g/m^2h)	Average relative humidity RH (%)	Average air temperature T_a (°C)	Average stone surface temperature T_s (°C)	Average dew point temperature T_d (°C)
1	1.7	141	84	77.9 ± 3.2	1.2 ± 0.3	−6.0 ± 0.3	−2.3 ± 0.8
2	2.7	219	81	86.8 ± 1.3	2.1 ± 0.1	−3.6 ± 0.1	0.1 ± 0.2
3	3.1	125	40	88.2 ± 3.5	2.0 ± 0.3	−1.4 ± 0.2	0.3 ± 0.8
4	2.8	187	68	78.3 ± 1.9	2.0 ± 0.1	−4.5 ± 0.1	−1.4 ± 0.3
5	3.8	188	50	71.1 ± 1.6	1.2 ± 0.2	−5.9 ± 0.2	−3.4 ± 0.4
6	3.2	234	74	75.8 ± 1.5	1.9 ± 0.1	−6.2 ± 0.1	−1.9 ± 0.3
7	4.6	141	31	59.9 ± 0.5	0.7 ± 0.0	−7.8 ± 0.0	−6.2 ± 0.1
8	18.8	297	16	58.9 ± 0.6	0.6 ± 0.1	−6.6 ± 0.1	−6.5 ± 0.1
9	23.6	750	32	62.9 ± 1.4	0.6 ± 0.1	−7.5 ± 0.1	−5.6 ± 0.3
10	22.3	453	20	64.5 ± 1.3	0.7 ± 0.0	−5.9 ± 0.0	−5.3 ± 0.3
11	18.7	438	23	74.2 ± 3.7	−16.4 ± 0.3	−24.2 ± 0.3	−20.0 ± 0.9
12	42.9	672	16	74.1 ± 3.2	−16.5 ± 0.3	−22.0 ± 0.3	−20.0 ± 0.8
13	21.5	375	17	73.7 ± 3.4	−16.6 ± 0.3	−22.3 ± 0.3	−20.1 ± 0.8
14	5.8	234	41	82.0 ± 1.0	−13.9 ± 0.3	−21.5 ± 0.2	−16.3 ± 0.2
15	4.0	204	51	91.4 ± 2.7	−13.5 ± 0.4	−21.3 ± 0.2	−14.7 ± 0.5

List of Figures

Fig. 1. Picture of experimental setup

Fig. 2. Sketch of experimental setup showing how humid air flows over the cold stone surface resulting in hoarfrost formation. Sensor 1 measures RH and T_a and is located 9 cm in front of the stone at a height of 2.5 cm above the stone surface. Sensor 2 measures T_s and is located at the corner of the stone. Sensor 3 measures wind speed and is located in front of the stone at a height of 1.5 cm.
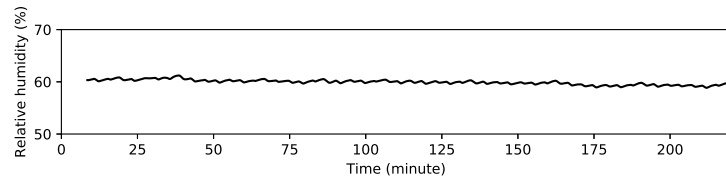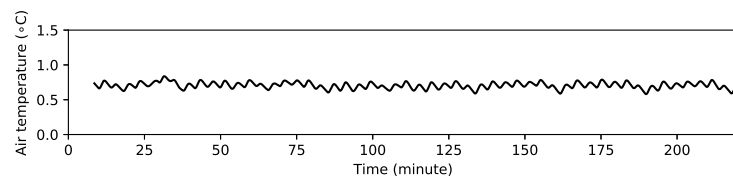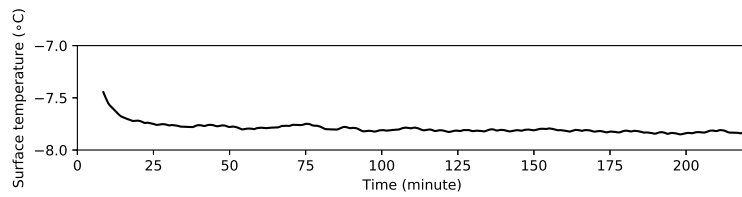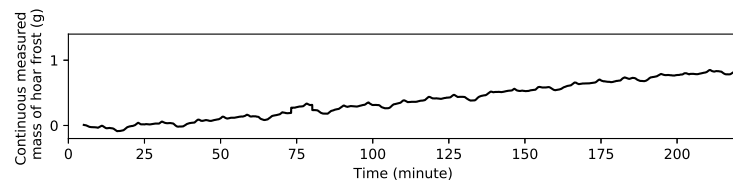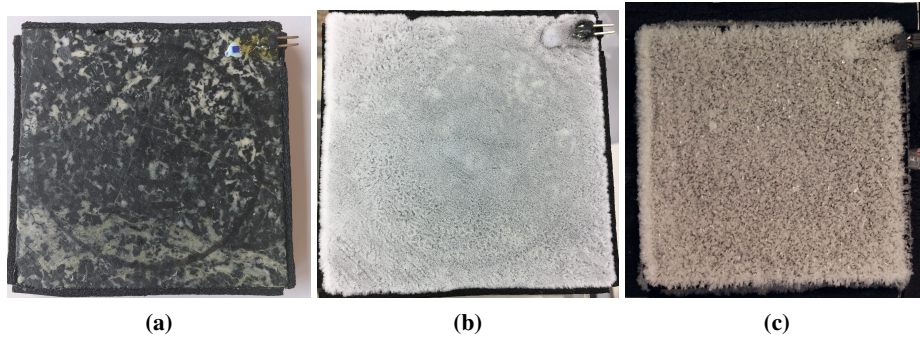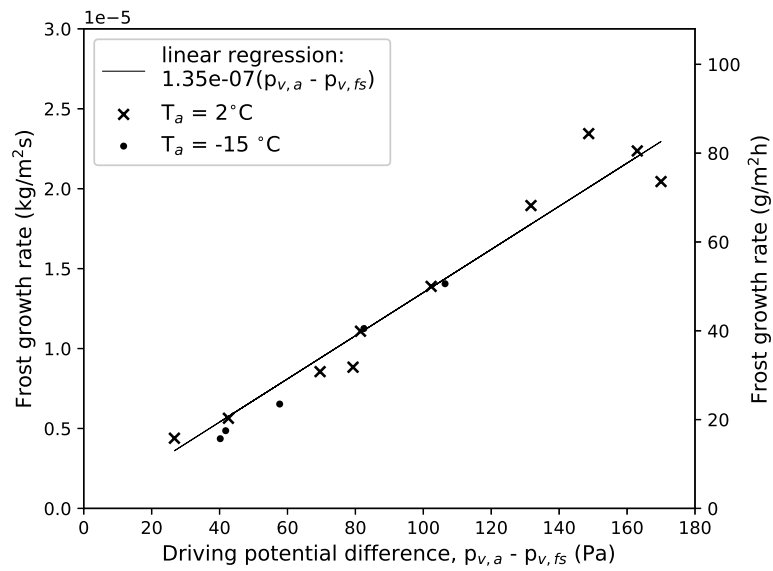
Fig. 3. Stability of measured parameters during test 7: (a) relative humidity, (b) air temperature, (c) surface temperature, (d) real time measured mass of hoarfrost, m_r.

(a)	**(b)**	**(c)**

Fig. 4. Image of (a) stone without hoarfrost, (b) frost growth at the end of test number 4, (c) frost growth at the end of test number 12.

Fig. 5. Frost growth rate as a function of the difference in the vapor pressure in the air and at the frost surface.

Paper II
The effect of anti-icing chemicals during hoar frost situations

This paper is awaiting publication and is not included in NTNU Open

Paper III
Chemical Frost Protection of Road Surfaces: A Laboratory Investigation

Fjærestad, J. S., Klein-Paste, A. and Wåhlin, J. (2020). Transportation Research Record: Journal of the Transportation Research Board

Research Article

Chemical Frost Protection of Road Surfaces: A Laboratory Investigation

Janne Siren Fjærestad[1], Alex Klein-Paste[1], and Johan Wåhlin[2]

Abstract
Anti-icing chemicals are commonly used to protect against hoar frost formation on roadways and bridges. Because of their negative impact on both environment and infrastructure, their use should be optimized. During conditions for hoar frost formation, this means that good knowledge is needed about when it is necessary to apply chemicals, and the corresponding protection time. A laboratory setup has been used to study the freezing process for a salted road surface during conditions for hoar frost formation, and a description of the process is given. It has been observed that freezing starts in the top layer of the applied solution, indicating the occurrence of a concentration gradient owing to accumulation of water molecules in the top layer. A British pendulum was used to simulate the mechanical load of traffic. The pendulum successfully destroyed the ice up to a certain ice fraction. This ice fraction was seen to depend on the amount of salt solution applied to the test sample. Finally, it has been illustrated how the maximum ice fraction can be used to calculate the amount of water allowed to be added to the road surface, and estimates of the protection time are given.

During winter time, roads and bridge decks can become slippery owing to hoar frost and this creates dangerous conditions for motorists (*1*). In Sweden in the winters of 2004–2005 and 2005–2006, 18.1% and 14.5% of accidents, respectively, occurred during hoar frost formation (*2*). Hoar frost growth occurs when water vapor in the air goes directly from gaseous state to solid state on a cold surface. For a surface without any anti-icing chemicals this can occur when the surface has a temperature below both the dew point temperature and the freezing temperature of water, $T_s < T_d$ and $T_s < 0$C.

Bridges have been found to cool more rapidly than adjacent roads, and are thus more vulnerable for hoar frost formation than adjacent roads (*3*). This has lead to fatal accidents (*4*). The Norwegian Public Roads Administration (NPRA) is planning for an upgrade of the E39 highway route at the westcoast of Norway. This includes replacing ferries by bridges for several fjord crossings along this route. Knowledge about how to avoid slippery roads owing to hoar frost formation on bridges is therefore valuable for the E39 project.

Chemicals like NaCl, MgCl$_2$ and CaCl$_2$ are commonly used to protect against hoar frost. They are often applied as solutions (brines) since liquids tend to adhere better to the road surface than granulates. Unfortunately, chemicals have a negative impact on the environment and can cause corrosion of the infrastructure (*5–7*) and their usage needs to be optimized. This means that, ideally, just enough chemical should be added to protect against slippery conditions while the conditions for hoar frost deposition are present. Winter maintenance practitioners are therefore interested in the protection time (longevity) of a given application. Predicting the protection time is challenging as it depends on many processes such as dilution owing to added moisture on the road surface, run-off and spray-off that can remove chemicals, and pavement temperature variations (*8*). The duration of hoar frost events also varies and little is known about how much hoar frost can form before the pavement becomes slippery. Currently road weather information systems (RWIS) typically can predict the duration of conditions for hoar frost to occur and there are micrometeorological models that incorporate the presence of anti-icing chemicals (*9, 10*). But, to the best of the authors' knowledge, there are no models in the public domain that predict the protection time of a given chemical application for a given hoar frost event. To support such development, a sound physical understanding is required of how and for how long chemicals protect against hoar frost formation.

[1]Norwegian University of Science and Technology, Trondheim, Norway
[2]Norwegian Public Roads Administration, Norway

Corresponding Author:
Janne Siren Fjærestad, janne.fjarestad@ntnu.no

The effect of anti-icing chemicals is often explained by the freezing point depression (*11*). The freezing point at a certain concentration for a given chemical can be found in a phase diagram, if such exists for the chemical in question. One source for freezing point depression data for common chemicals is the *CRC Handbook of Chemistry and Physics* (*12*). For the process of hoar frost formation water is added to the road surface by humidity transport from the air, continuously diluting the concentration of any chemical present on the road surface. This raises the freezing temperature. At a certain point the freezing temperature exceeds the surface temperature, and freezing is expected to start.

In this laboratory investigation two fundamental questions are addressed relating to hoar frost formation when the applied anti-icing chemical has been diluted to its freezing concentration: 1) how does hoar frost or ice accumulate when the freezing point of the solution has reached the surface temperature, and 2) when does the accumulation of hoar frost/ice start to cause slippery conditions?

Theory

The time it takes from when the anti-icing chemical is applied to when the road gets slippery can be seen as the protection time for the anti-icing measure. It is proposed that this process can be divided into two parts: 1) the dilution process when water is added to the applied solution owing to humidity transport from the air, and 2) the freezing process. The dilution process lasts from when the anti-icing chemical is applied until the freezing concentration is reached, then the freezing process starts and lasts until the road gets slippery.

The rate of humidity transport between the air and the road surface is given as (*13*):

$$\dot{m} = K_p(p_{v,a} - p_{v,s}) \qquad (1)$$

where K_p is the mass transfer coefficient based on the vapor pressure difference, $p_{v,a}$ is the water vapor pressure in the air and $p_{v,s}$ is the water vapor pressure at the road surface. For a clean surface without any chemicals, the water vapor pressure at the surface is given as the saturation water vapor pressure at the surface temperature, $p_{v,s} = p_v^{sat}(T_s)$, where T_s is the surface temperature. When an anti-icing chemical is applied to the surface, the water vapor pressure at the surface is given as water vapor pressure above the present solution, $p_{v,s} = p_v^{sol}$. To determine the water vapor pressure above the solution it is useful to introduce the water activity, a_w. The water activity is often described as the amount of free water not bound to any dissolved chemicals. The water activity of a solution is defined as (*14*):

$$p_v^{sol} = a_w^{sol} p_v^{water} \qquad (2)$$

where p_v^{water} is the water vapor pressure over pure water at the solution temperature. The water activity ranges from 0 for a solution with no free water to 1 for pure water. As described by Wåhlin et al. the water activity can be found by using the Extended UNIQUAC model which is valid from the freezing points of the solutions to 100°C (*15, 16*). Similarly to Equation 2 the water activity of ice, p_c^{ice}, is given as (*14*):

$$p_v^{ice} = a_w^{ice} p_v^{water} \qquad (3)$$

where p_v^{water} is the water vapor pressure over pure water at the ice temperature.

For wet pavement anti-icing it has been reported that a much lower salt concentration than that found from the freezing curve is enough to keep the friction at acceptable levels (*17, 18*). This is explained by anti-icing chemicals reducing the mechanical strength of the ice forming, allowing the traffic to destroy the ice. This allows the tires to get in direct contact with the pavement, and sufficient friction is obtained. Klein-Paste and Wåhlin found that a brine fraction of $F_{b,min} = 0.4$ was sufficient to ensure mechanical load to destroy the ice (*18*). This means that an ice fraction of $F_{ice,max} = 0.6$ is allowed without reducing the friction. For the system of an anti-icing chemical and water, ice and solution can coexist for temperatures above and concentrations below the eutectic point. The ice fraction describes the amount of ice present in the system, that is the mass of ice divided by the total mass of ice and solution. The ice fraction can be found from the phase diagram of NaCl using the lever rule:

$$F_{ice}(T) = 1 - \frac{c}{c_f(T)} \qquad (4)$$

where c is the calculated concentration of the solute on the stone surface, that is the mass of added chemical divided by the total mass of chemical and water. $c_f(T)$ is the freezing concentration at the surface temperature. Hence $F_{ice} = 0$ means that everything is liquid and $F_{ice} = 1$ means that everything is frozen. The process of hoar frost formation differs from the experiment performed by Klein-Paste and Wåhlin by the continous addition of water to the system, owing to the humidity transport between air and road surface (*18*). Determining a maximum ice fraction for hoar frost formation will make it possible to determine the maximum amount of humidity allowed to be transported to the road surface without getting slippery driving conditions.

Method

Hoar Frost Growth on a Salted Surface

The experiment was performed by the use of a setup designed to simulate typical conditions for hoar frost

formation on road surfaces. The setup consists of an open loop wind tunnel, where humid air flows over a cold stone surface of 8×8 cm. Water vapor is added to the air by a water bath, the air flow is driven by a tangential fan and the stone is cooled by Peltier elements. The air velocity can be controlled within the range from 0.6 m/s to 1.2 m/s, relative humidity (RH) within the range from 60% to 100% and the surface temperature can be set from air temperature to 8°C below air temperature. More details about the setup will be published elsewhere (*19*).

In the presence of any anti-icing chemical, the moisture added to the surface stays in liquid form until the freezing point is reached. To avoid run-off of the liquid solution, a 1 mm thick silicon rim was attached along the edges of the stone. The remaining area for application of salt solution was 45.5 cm^2. The setup was placed inside a walk in cold laboratory with $T_a = 2°C$. The surface temperature was set to approximately –5°C and the RH was set to approximately 85%. The RH, the air temperature, T_a, and the stone surface temperature, T_s, were measured during all tests and logged with a frequency of 2.4 Hz. The wind was 0.6 m/s for all tests.

A (pre-diluted) NaCl solution ($T_f = -6.4$ °C) was chosen as the anti-icing agent. By applying a solution with T_f close to T_s, the process of dilution before c_f was reached was reduced to a minimum. This made it possible to isolate only the freezing process. The tests were performed by applying about 0.3 or 0.5 ml 10% NaCl solution on the stone surface. The amount of applied solution was determined by weighing the stone before and after applying the salt solution. The salt solution was spread evenly over the surface by use of a glass plate. The tests started when the stone cooling system was turned on. The length of each test was determined based on a combination of visual judgement and weighing, to achieve a range of different ice fractions. 18 tests were performed, 12 with approximately 0.3 g of applied salt solution and 6 with approximately 0.5 g of applied salt solution. This correspond to film thicknesses of 0.06 mm and 0.1 mm respectively for the two series. In Norway it is recommended to use $20 - 40$ g/m^2 of 23% NaCl solution during conditions for hoar frost formation (*20*). This corresponds to $4.6 - 6.9$ g/m^2 NaCl. The amounts of NaCl used for the two film thicknesses in this study (6.6 g/m^2 and 11.0 g/m^2) are in this range.

A camera was placed at a low angle towards the test sample and photos were taken every minute during the tests. A light source was placed in the back of the sample to produce reflections, thus making it possible to see the surface of the solution. The images taken during the tests were studied to determine two different transitions in the frost growth process: (a) the point when the first ice crystals were observed in the salt solution, and (b) the point

when the first small, white hoar frost crystals were observed on the frozen surface of the salt solution. The mass of moisture added to the stone surface by condensation and deposition were measured by weighing the stone before and after the hoar frost growth tests.

At the start of the test the rate of water molecules transported from the air to the solution was found by combining Equations 1 and 2:

$$\dot{m} = K_p(p_v^a - (a_w^{sol} p_v^{water})) \tag{5}$$

where K_p is the mass transfer coefficient based on the vapor pressure difference, p_v^a is the water vapor pressure in the air flow, a_w^{sol} is the water activity of the solution and p_v^{water} is the water vapor pressure over pure water.

At the end of the test, when the entire surface was covered with ice crystals, the rate of water molecules transported to the surface was given as:

$$\dot{m} = K_p(p_v^a - (a_w^{ice} p_v^{water})) \tag{6}$$

where a_w^{ice} is the water activity of ice.

For a 10 wt % solution of NaCl at –5°C the water activity of the solution, a_w^{sol}, is 0.93. The water activity of ice at the same temperature, a_w^{ice}, is 0.95. Owing to this small difference, the rate of water transported to the surface was assumed constant during the experiments. This allowed the calculation of the amount of added water (and thereby F_{ice}) during the experiment from interpolating the measured mass before and after the experiment.

Mechanical Strength of Hoar Frost

A British Pendulum Tester was used to test the mechanical strength of the hoar frost present on the stone surface after the frost growth periods (*21*). To avoid melting prior to the pendulum test, the pendulum was placed inside a neighboring cold room. Here the air temperatur was -5°C, which is close to the stone surface temperature. The width of a standard rubber block was reduced to 40 mm to ensure the block did not touch the silicon rim and the temperature sensor. The hoar frost from each test run was exposed to five pendulum passes before the sliding track was studied visually. The amount of hoar frost removed was found for each test. Similar to the procedure of Klein-Paste and Wåhlin (*18*), levels of <25%, 25–75% and >75% of hoar frost removed after five pendulum passes were classified as being "intact", "partly removed" and "removed", respectively. All pendulum tests were performed on samples with a distinct layer of hoar frost. Figure 1 shows images of two different hoar frost samples after five pendulum passes. In (*a*) the hoar frost layer was intact after five pendulum passes, while in (*b*) the hoar frost layer was removed after five pendulum passes.
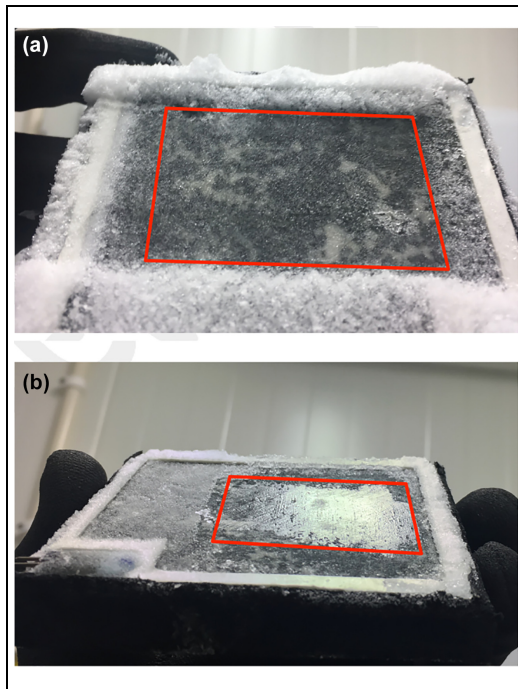
Figure 1. Image of hoar frost samples after five pendulum passes for (*a*) a test where the hoar frost was intact (0% removed) and (*b*) a test where 95% of the hoar frost was removed by the pendulum. The area where the pendulum is in contact with the stone surface is marked with red.

Results

Hoar Frost Growth

For the 18 tests performed, RH ranged between 78% and 92%, T_s ranged between –4.8°C and –6.1°C and T_a ranged between 1.2°C and 1.7°C. Within each test, the RH was stable within ± 2 %, T_a within ± 0.2°C and T_s within ± 0.2°C. Figure 2 shows photos taken during different stages of the freezing process. Initially the entire surface was covered with liquid salt solution, shown in Figure 2*a*. The freezing always started with frozen crystals floating on top of the solution, even though the system is cooled from below. Figure 2*b* shows this second stage where ice crystals start to appear in the salt solution. This is seen as small lines in the reflection from the light. The ice crystals continued to form on top of the solution until the entire surface was covered with ice, seen in Figure 2*c*. By touching the frozen layer of ice with a glass plate, it was observed that liquid brine was present below the frozen layer. The start of hoar frost formation on top of the frozen layer was seen by less reflections and
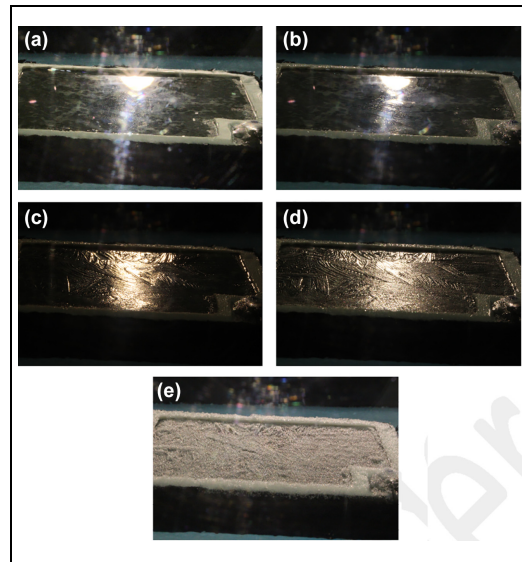

Figure 2. Development of hoar frost formation on surface with anti-icing chemical: (*a*) Only liquid salt solution, (*b*) First observable frozen crystals floating on the top of the liquid, (*c*) Frozen crystals cover the entire surface with liquid salt solution below, (*d*) Early stage of hoar frost formation on top of the frozen layer, and (*e*) Surface completely covered with hoar frost.

a whiter surface. Figure 2*d* shows an early stage of this hoar frost formation. The hoar frost dendrites continued to grow until the experiment was terminated. Figure 2*d* shows a distinct layer of hoar frost covering the entire surface. The further development of ice below the first observed frozen layer was not possible to study visually. However, the pendulum tests revealed that after a certain time the liquid layer disappeared and the ice adhered to the stone surface.

The first observable ice crystals occurred at a mean ice fraction of 0.19 with a 95% confidence intervals of [0.10 0.26]. No difference was seen between the two applied film thicknesses for the ice fraction at which the first frozen ice crystals were observed. The mean amount of humidity added to the test sample when the first ice crystal was observed was 0.15 and 0.22 g for the two film thicknesses of 0.06 mm and 0.1 mm. This corresponds to 33.3 and 44.4 g/m ^{2}.

The first observable hoar frost on top of the frozen layer occurred for a mean ice fraction of 0.44 and 0.37 two film thicknesses of 0.06 mm and 0.1 mm. The corresponding 95% confidence intervals were [0.36 0.52] and [0.29 0.44]. The mean amount of humidity added to the test sample was 0.35 g for the film thickness of 0.06 mm and 0.39 g for the film thickness of 0.1 mm. This
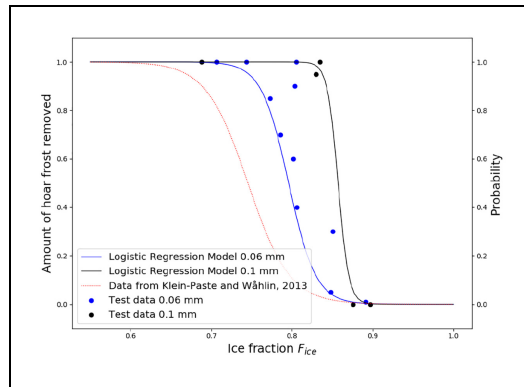
Figure 3. Left y-axis: Amount of hoar frost removed after five pendulum passes for the applied film thicknesses of 0.06 mm (blue dots) and 0.1 mm (black dots) for different ice fractions F_{ice}. Right y-axis: Probability of removal of hoar frost as a function of ice fraction F_{ice} for 0.06 mm applied film (blue line) and 0.1 mm applied film (black line) . Dotted red line show data from Klein-Paste and Wåhlin (*18*).

corresponds to 77.8 g/m^2 and 87.8 g/m ^{2}. The small difference between the ice fraction at which hoar frost was observed for the two film thicknesses was not found to be statistically significant when using the one-way Anova test.

Mechanical Strength of Hoar Frost

Figure 3 shows the amount of removed ice plotted against the ice fraction F_{ice} for all pendulum tests. Blue dots are representing the tests with applied film thickness of 0.06 mm and black dots are representing the tests with film thickness of 0.1 mm.

Logistic regression of the tests categorized as "intact" and "removed" was performed by the use of the Scikit-learn machine learning library for Python. This calculated the probability of removal of the hoar frost as a function of the ice fraction, F_{ice}:

$$p(F_{ice}) = \frac{1}{1 + e^{-(\beta_0 + \beta_1 F_{ice})}} \qquad (7)$$

where β_0 and β_1 are the linear fitting coefficients. The threshold for successful ice removal was set to more than 75% of the ice removed. The tests categorized as "partly removed" (25–75% of hoar frost removed) were therefore treated as "intact" in the logistic regression. The probability of successful removal of the hoar frost for different ice fractions as determined by the logistic regression is also shown in Figure 3 for the two test series.

It is seen that by applying a thicker film of brine, a higher ice fraction is allowed for a certain probability of

hoar frost removal than for a thinner film thickness. This means that a thicker film allows a larger amount of water transported from the air to the surface for each gram of NaCl applied than a thinner film, without becoming slippery.

Klein-Paste and Wåhlin have studied the mechanical strength of frozen salt solutions without any addition of humidity from the air (*18*). Their calculated probability of ice removal from laboratory tests is shown with dotted red line in Figure 3. It is seen that a higher ice fraction is allowed during hoar frost conditions than for freezing without humidity transport.

From the regression it was found that for the applied film thickness of 0.06 mm the 99.9% probability of sufficient ice removal occurs at $F_{ice} = 0.67$. For a surface temperature of –5°C, an ice fraction of 0.67 ($p = 0.999$) corresponds to a salt concentration of 2.6%. This occurs after an added amount of 0.84 g of moisture from the air to the test sample.

For the series of 0.1 mm applied film thickness it is seen that the 99.9% probability of sufficient ice removal occurs at $F_{ice} = 0.81$. For a surface temperature of –5°C, an ice fraction of 0.81 ($p = 0.999$) corresponds to a salt concentration of 1.5%. This occurs after an added amount of 2.80 g of moisture from the air to the test sample.

Discussion

The Freezing Process

The first ice crystals were observed when the ice fraction was well above 0 ($\bar{F}_{ice} = 0.19$). This could be owing to supercooling of the solution since there was no seeding initiating the freezing process. It could also be that it was not possible to detect the first ice crystals as soon as they appeared. Since heat is extracted below it is expected that the stone surface is colder than the top surface of the brine film. Nevertheless, the freezing always started from the top, with liquid solution being present below the ice. This indicates that there is a concentration gradient in the brine film. This is likely because the diffusion coefficient for water vapor in air, ($\sim 10^{-5}$ m^2/s), is five orders of magnitude larger than the diffusion coefficient for water in salt solutions, ($\sim 10^{-10}$ m^2/s) (*22, 23*). The result is an accumulation of water molecules in the top layer which leads to a higher freezing temperature in the top layer than in the bottom layer of the solution. The solution of anti-icing chemicals thereby continues to protect against slippery conditions even when ice starts to form on top of the solution.

There was no significant difference in the amount of humidity added to the surface of the 0.06 mm and 0.11 mm film until the first hoar frost crystals were observed. This is also an indication that there is a

concentration gradient in the solution. If the added water molecules were homogeneously distributed in the solution, it would require (almost) double the amount of humidity added to the 0.11 mm film compared with the 0.06 mm film before the entire surface was covered with ice, and hoar frost was observed.

After a large enough humidity transport, it was observed by the pendulum that frozen ice was stuck to the stone surface. This indicates that the diffusion of water molecules towards the colder road surface continues also after the surface is entirely covered with ice. Owing to this diffusion, the liquid layer below the ice layer continues to dilute until the freezing temperature is reached also for the solution closest to the stone surface. The remaining solution is probably captured inside small pockets in the ice layer, similarly to the observations done by Klein-Paste and Wåhlin (*18*).

Mechanical Strength of Hoar Frost

The mechanical action of the pendulum was able to remove the ice up to a certain ice fraction. After this point the diffusion of water molecules down to the salt solution had reduced the concentration sufficiently for ice to form also in the bottom of the salt solution. The ice therefore adhered to the stone surface. Successful removal of hoar frost and ice owing to mechanical exposure is explained to be important for cars to obtain sufficient friction (*18*). The maximum ice fraction at which the ice was removed successfully can therefore be used to calculate the amount of water allowed to be added to a salted road surface before it becomes slippery during hoar frost formation. This information is valuable to optimize the usage of chemicals during hoar frost formation.

It was found that by applying a thicker film of brine, a higher ice fraction is allowed for a given probability of hoar frost removal than for a thinner film thickness. This could possibly be explained by the diffusion of water in the salt solution. At a given ice fraction, the liquid layer below the ice layer is thicker for higher film thicknesses. This makes the diffusion process for water molecules down to the stone surface slower for higher film thicknesses, resulting in higher allowed ice fractions until ice adhered to the surface. Using other chemicals like $MgCl_2$ and $CaCl_2$ with lower diffusivity in water (*23*) could possibly extend the protection time during hoar frost formation.

The higher allowed ice fraction reported here compared with the tests by Klein-Paste and Wåhlin might be explained by the occurrence of a frozen layer with liquid solution below (*18*). Parts of the humidity transported to the system after the occurrence of this layer will be kept as hoar frost on top of the ice. This hoar frost will add water to the system and raise the ice fraction without actually diluting the solution below the ice layer. Using the criterion $F_{ice} = 0.6$ proposed by Klein-Paste and Wåhlin is therefore a conservative criterion during hoar frost formation (*18*).

The presented laboratory setup and test method does not take into account how exposure of traffic will influence the freezing of the salt solution. The traffic will probably enhance the mixing of the added water and the salt solution, reducing the concentration gradient. The situation will then be more similar to the freezing of a homogeneous solution studied by Klein-Paste and Wåhlin, and their proposed $F_{ice} = 0.6$ should therefore be valid also during hoar frost formation (*18*). However, this traffic-induced mixing is probably not that effective in the area between the wheel tracks. Keeping good friction is also important for this area.

Implications for Calculation of Hoar Frost Protection Time

One of the critical questions when predicting the protection time for an applied anti-icing chemical during hoar frost formation is how much humidity is allowed to be transported from the air to the road surface. A very conservative criterion is to keep the concentration of anti-icing chemical above the freezing concentration, c_f. This corresponds to an ice fraction $F_{ice} = 0$. However, the presented pendulum tests have shown that an ice fraction up to 0.81 can be removed by the mechanical load of the pendulum with 99.9% probability. So allowing only humidity to accumulate until the solution starts to freeze is likely to be over-conservative. The protection time in real situations also depends on the rate of the humidity transport, Equation 1. All weather variables like air temperature, air humidity, wind speed and surface temperature influence this mass transport rate. In addition, a mass transfer coefficient representative for the specific road site has to be determined.

To illustrate the effect of the chosen criterion before the road gets slippery, the protection time was calculated for four different cases, shown in Table 1. Two different amounts of 23% NaCl solution were chosen to correspond to the amounts of NaCl used in the presented laboratory experiment. Cases 1 and 3 use $F_{ice} = 0$ as criterion. Cases 2 and 4 use the ice fraction at which the ice was removed by the pendulum with 99.9% probability as criterion. A field study has been performed by Karlsson in Sweden during three winter seasons (*24*). Reported amounts of hoar frost deposited during one night are in the range from 55 to 495 g/m^2, with an average of approximately 150 g/m^2. Assuming one night to be 12 h, this corresponds to an average of 12.5 g/m^2h. The calculations are based on this rate of humidity

Table 1. Calculation of Amount of Added Water Allowed and Protection Time for Four Different Cases. Calculations are Based on an Assumed Amount of Humidity Transport of 12.5g/m²h

Case	Applied 23% NaCl solution (g/m²)	Applied NaCl (g/m²)	Criterion F_{ice}	Water allowed to be added (g/m²)	Protection time (h)
1	28.5	6.6	0	54	4.3
2	28.5	6.6	0.67	222	17.8
3	48	11.0	0	92	7.4
4	48	11.0	0.81	688	55.0

transport and a surface temperature of $-5\,°C$. For simplicity, it is assumed that the rate of humidity transport is constant throughout the entire process for the protection time calculation.

It is seen that by allowing an ice fraction of 0.67, four times more water can be added to the road surface compared with an ice fraction of 0 for the lowest application rate. For the higher application rate an ice fraction of 0.81 allows more than seven times more water to be added compared with an ice fraction of 0. In Case 2 each applied gram of NaCl allows 33.6 g of water to be transported to the surface. In Case 4 each applied gram of NaCl allows 62.5 g of water to be transported to the surface. This difference is a consequence of the larger allowed ice fraction for the highest applied amount of NaCl.

Conclusion

The presented laboratory investigation has shown that a salt solution diluted by humidity transport from the air started to freeze from the top. This is explained by the slower diffusion of water molecules in the solution than in the air, resulting to a concentration gradient with the lowest salt concentration in the top layer.

It was shown that the time a certain amount of anti-icing agent protects a surface from becoming slippery owing to hoar frost formation is under-estimated when using the freezing curve. The allowed ice fraction was found to be dependent on the thickness of the applied brine film. For a 0.06 mm thick film of 10% NaCl the pendulum will remove the ice with 99.9% probability for an ice fraction of 0.67. For a 0.1 mm thick film of 10% NaCl the pendulum will remove the ice with 99.9% probability for an ice fraction of 0.81.

Further work should include studies with other chemicals like $MgCl_2$ and $CaCl_2$ to determine how different diffusivities affect the freezing process and the protection time. Field tests should be performed to further examine the process of hoar frost formation with the presence of practical issues such as salt losses and traffic.

Author Contributions

The authors confirm contribution to the paper as follows: study conception and design: J. S. Fjærestad, A. Klein-Paste, J. Wåhlin; data collection: J. S. Fjærestad; analysis and interpretation of results: J. S. Fjærestad, A. Klein-Paste, J.Wåhlin; draft manuscript preparation: J. S. Fjærestad, A. Klein-Paste, J. Wåhlin. All authors reviewed the results and approved the final version of the manuscript.

References

1. Norrman, J., M. Eriksson, and S. Lindqvist. Relationships Between Road Slipperiness, Traffic Accident Risk and Winter Road Maintenance Activity. *Climate Research*, Vol. 15, 2000, pp. 185–193.
2. Andersson, A., and L. Chapman. The Use of a Temporal Analogue to Predict Future Traffic Accidents and Winter Road Conditions in Sweden. *Meteorological Applications*, Vol. 18, No. 2, 2011, pp. 125–136. https://doi.org/10.1002/met.186.
3. Knollhoff, D. S., E. S. Takle, W. A. Gallus, Jr., and D. Burkheimer. Use of Pavement Temperature Measurements for Winter Maintenance Decisions. *Proc., Transportation Conference*, U.S. Department of Transportation, Washington, D.C., pp. 33–36.

4. Statens Havarikommisjon for Transport. Rapport om møteulykke mellom vogndtog og to personbiler på E16 i Flåm 16. november 2007. Technical Report. Statens Havarikommisjon for Transport, 2010.

5. Ramakrishna, D. M., and T. Viraraghavan. Environmental Impact of Chemical Deicers – A Review. *Water, Air, and Soil Pollution*, Vol. 166, No. 1, 2005, pp. 49–63. https://doi.org/10.1007/s11270-005-8265-9.

6. Fay, L., and X. Shi. Environmental Impacts of Chemicals for Snow and Ice Control: State of the Knowledge. *Water, Air, & Soil Pollution*, Vol. 223, No. 5, 2012, pp. 2751–2770. https://doi.org/10.1007/s11270-011-1064-6.

7. Xu, G., and X. Shi. Impact of Chemical Deicers on Roadways Infrastructure: Risks and Best Management Practices. In *Sustainable Winter Road Operations* (X. Shi, and L. Fu, eds.), John Wiley & Sons, Hoboken, N.J., 2018.

8. Lysbakken, K. R., and H. Norem. Processes that Control Development of Quantity of Salt on Road Surfaces after Salt Application. *Transportation Research Record: Journal of the Transportation Research Board*, 2011. 2258: 139–146.

9. Denby, B. R., I. Sundvor, C. Johansson, L. Pirjola, M. Ketzel, M. Norman, K. Kupiainen, M. Gustafsson, G. Blomqvist, M. Kauhaniemi, and G. Omstedt. A Coupled Road Dust and Surface Moisture Model to Predict Non-Exhaust Road Traffic Induced Particle Emissions (NOR-TRIP). Part 2: Surface Moisture and Salt Impact Modelling. *Atmospheric Environment*, Vol. 81, 2013, pp. 485–503.

10. Fujimoto, A., R. Tokunaga, M. Kiriishi, Y. Kawabata, N. Takahashi, T. Ishida, and T. Fukuhara. A Road Surface Freezing Model Using Heat, Water and Salt Balance and its Validation by Field Experiments. *Cold Regions Science and Technology*, Vol. 106, 2014, pp. 1–10.

11. Atkins, P., and J. D. Paula. *Physical Chemistry*, 9th ed. Oxford University Press, 2006.

12. Rumble, J. R. (ed.). *CRC Handbook of Chemistry and Physics*, 100th ed. CRC Press, Boca Raton, 2019.

13. Webb, RL. Standard Nomenclature for Mass Transfer Processes. *International Communications in Heat and Mass Transfer*, Vol. 17, No. 5, 1990, pp. 529–535. https://doi.org/10.1016/0735-1933(90)90001-Z.

14. Koop, T. The Water Activity of Aqueous Solutions in Equilibrium with Ice. *Bulletin of the Chemical Society of Japan*, Vol. 75, 2002, pp. 2587–2588.

15. Wåhlin, J., J. S. Fjærestad, K. Thomsen, and A. Klein-Paste. Thermodynamics of Deicing Chemicals. Presented at 96th Annual Meeting of the Transportation Research Board, Washington, D.C., 2017.

16. Thomsen, K. Modeling Electrolyte Solutions with the Extended Universal Quasichemical (Uniquac) Model. *Pure and Applied Chemistry*, Vol. 77, 2005, pp. 531–542.

17. Haavasoja, T., J. Nylander, and P. Nylander. Relation of Road Surface Friction and Salt Concentration. *Proc., 16th SIRWEC Conference*, Helsinki, Finland, 2012.

18. Klein-Paste, A., and J. Wåhlin. Wet Pavement Anti-Icing - A Physical Mechanism. *Cold Regions Science and Technology*, Vol. 96, 2013, pp. 1–7.

19. Fjærestad, J. S., J. Wåhlin, and A. Klein-Paste. Experimental Setup Simulating Hoar Frost Formation on Roadways. *Journal of Cold Regions Engineering*, Accepted for publication 2019.

20. *Usage of Salt (in Norwegian)*. D2-ID9300a-7 ed. Norwegian Public Road Administration, 2017.

21. Giles, C. G., B. E. Sabey, and K. H. F. Cardew. *Development and Performance of the Portable Skid-Resistance Tester*. Technical Report 66. Road Research Laboratory, London, 1964.

22. Bolz, R. E., and G. L. Tuve GL. *CRC Handbook of Tables for Applied Engineering Science*, 2nd ed. CRC Press, Boca Raton, 1973.

23. Wåhlin, J., and A. Klein-Paste. The Effect of Mass Diffusion on the Rate of Chemical Ice Melting Using Aqueous Solutions. *Cold Regions Science and Technology*, Vol. 139, 2017, pp. 11–21.

24. Karlsson, M. Prediction of Hoar-Frost by Use of a Road Weather Information System. *Meteorological Applications*, Vol. 8, No. 1, 2001, pp. 95–105.

Paper IV
Thermodynamics of deicing chemicals